Chemistry of *C*-Trimethylsilyl-Substituted Heterocarboranes. 21. Syntheses, Structures, EPR Spectra, and Reactivities of Bent-Sandwich and Half-Sandwich Titanacarboranes. Full Analysis of Spin−Spin Coupling in Two Structurally Characterized Titanium(III)−Carborane Dimers

Narayan S. Hosmane,*,† Ying Wang, Hongming Zhang, Kai-Juan Lu, John A. Maguire, Thomas G. Gray, and Karen A. Brooks

Department of Chemistry, Southern Methodist University, Dallas, Texas 75275

Eberhard Waldhör and Wolfgang Kaim

Institut für Anorganische Chemie, Universität Stuttgart, Pfaffenwaldring 55, 70569 Stuttgart, Germany

Reinhard K. Kremer

Max-Planck-Institut für Festkörperforschung, Heisenbergstrasse 1, 70506 Stuttgart, Germany

Received October 22, 1996[⊗]

The reaction of Cp_2TiCl_2 with the unsolvated dilithium compounds *closo-exo*-Li-1-Li-2-(R)-3-($SiMe_3$)-2,3-$C_2B_4H_4$ (R = $SiMe_3$, Me, H) produced dimeric mixed-ligand sandwich titanacarboranes [*commo*-1-Cp-1-Ti(III)-2-(R)-3-($SiMe_3$)-2,3-$C_2B_4H_4$]$_2$ (R = $SiMe_3$ (**1**), Me (**2**), H (**3**)) in yields of 60%, 54%, and 60%, respectively. The chemical oxidation of these titanacarboranes in the presence of $TiCl_4$ in THF resulted in the formation of the corresponding diamagnetic Ti(IV) species 1-(Cp)-1-(Cl)-1-(THF)-1-Ti-2-(R)-3-($SiMe_3$)-2,3-$C_2B_4H_4$) (R = $SiMe_3$ (**7**), Me (**8**), H (**9**)) in 86%, 58%, and 45% yields, respectively. When the bis(trimethylsilyl)-substituted dilithiacarborane precursor was reacted with $TiCl_3$, only the monomeric full-sandwich chlorotitanacarborane [Li(TMEDA)]$_2$[1-Cl-1,1′-Ti-(2,3-($SiMe_3$)$_2$-2,3-$C_2B_4H_4$)$_2$] (**4**) was produced, while replacement of a $SiMe_3$ group with a less sterically demanding Me group afforded the dimeric titanacarborane [Li(TMEDA)]$_2$[1,1′-Ti-(2-Me-3-$SiMe_3$-2,3-$C_2B_4H_4$)$_2$]$_2$ (**5A**). On the other hand, when the TMEDA-solvated *closo-exo*-4,5-[(μ-H)$_2$Li(TMEDA)]-1-Li[(TMEDA)-2,4-($SiMe_3$)$_2$-2,4-$C_2B_4H_4$ was the precursor, reaction with $TiCl_3$ yielded only the corresponding monomeric half-sandwich chlorotitanacarborane 1-(TMEDA)-1-Cl-1-Ti(III)-2,4-($SiMe_3$)$_2$-2,4-$C_2B_4H_4$ (**6**). In addition to the X-ray analyses of **1**, **5A**, **6**, and **7**, the Ti(III) compounds and an electrochemically generated Ti(IV)/Ti(III) mixed-valence complex (**5B**) were characterized by EPR spectroscopy. The dimers **1** and **5A** exhibit unusually well-resolved triplet EPR features, which were fully analyzed and correlated with the structural results. Magnetic susceptibility measurements reveal a rather small d^1-d^1 exchange coupling constant of -45.8 cm^{-1} (antiferromagnetic interaction) for **1**. The one-electron oxidation of **5A** produced an anion ($S = {}^1/_2$) with rhombic EPR features, which was tentatively identified as a delocalized [Ti(+3.5)]$_2$ mixed-valence species (**5B**).

Introduction

The group 4 (titanium group) organometallic compounds have been the subject of numerous structural, spectroscopic and synthetic investigations.[1] Of these compounds, the half- and full-sandwich complexes of Ti(III) and Ti(IV) with ligands in the cyclopentadienide system $[C_5R_5]^-$ (R = H[Cp], Me[Cp*], or some other alkyl or aryl group) have received the most attention. Interest in the d^0 Ti(IV) complexes has been generated by their use in Ziegler−Natta olefin polymerization catalytic systems.[2,3] On the other hand, the d^1 Ti(III) complexes, while having their own unique chemistry, are of special interest in that their dinuclear complexes [(Cp_2Ti)$_2$XY] (X and Y = bridging ligands) are among the simplest model compounds for studying spin−spin interactions.[4] Interest in the design of novel molecular magnetic materials[5] has made the study of electron spin−electron spin interactions in dinuclear and poly-

† Camille and Henry Dreyfus Scholar.

⊗ Abstract published in *Advance ACS Abstracts,* March 1, 1997.

(1) For general references, see: *Comprehensive Organometallic Chemistry II*; Abel, E. W., Stone, F. G. A., Wilkinson, G., Eds.; Elsevier Science Ltd.: Oxford, England, 1995; Vol. 4.

(2) Cardin, D. J.; Lappert, M. F.; Raston, C. L. *Chemistry of Organo-Zirconium and -Hafnium Compounds*; Ellis Horwood, Ltd.: West Sussex, England, 1986.

(3) Jordan, R. F. *J. Chem. Educ.* **1988**, *65*, 285. Jordan, R. F.; Bradley, P. K.; LaPointe, R. E.; Taylor, D. F. *New J. Chem.* **1990**, *14*, 505.

(4) Corbin, D. R.; Atwood, J. L.; Stucky, G. D. *Inorg. Chem.* **1986**, *25*, 98 and references cited.

(5) Miller, J. S.; Epstein, A. J. *Angew. Chem.* **1994**, *106*, 399; *Angew. Chem., Int. Ed. Engl.* **1994**, *33*, 385.

S0276-7333(96)00890-4 CCC: $14.00

nuclear transition metal complexes a topic of intense research.[6−8] However, only a relatively small number of symmetrical Ti(III) dimers have been completely characterized by EPR, magnetic susceptibility measurements, and crystal structure determinations.[9,10] Interactions of the metal-centered unpaired electrons in these compounds led to EPR spectra typical of triplet ($S = 1$) states. Together with the magnetic susceptibility data, a thorough analysis of well-resolved EPR spectra can provide unique insights into the interaction between the two unpaired electrons.

The *nido*-carborane dianions of the type $[R_2C_2B_9H_9]^{2-}$ or $[R_2C_2B_4]^{2-}$ (R = H or a cage-carbon substituent) offer attractive alternatives to the $[C_5R_5]^-$ ligands. Studies have shown that these dianions act as six-electron π donors and a chemistry strikingly parallel to that of the metallocenes has been developed.[11] Recently, Jordan and co-workers have shown that the d^0, mixed-ligand, bent-sandwich complexes of the type $[(Cp^*)M(R)(C_2B_9H_{11})]$ and $[(Cp^*)M(R)(L)(C_2B_9H_{11})]$ (M = Ti, Zr, Hf; R = Me, Et; L = labile ligand) exhibit some catalytic activity and undergo selective insertion and amine elimination reactions.[12] Much less information is available on the smaller cage complexes; Grimes and co-workers have synthesized bent-sandwich complexes of the mixed C_2B_4−carborane and Cp ligands, Cp′MXY-$(R_2C_2B_4H_4)$ (M = Ti, Zr, Hf, Nb, Ta; R = $SiMe_3$, Me, Et; Cp′ = Cp or Cp*; X, Y = Cl, alkyl, aryl, C_4H_8O (THF)), with structures of the niobium and tantalum species being reported.[13] However, the only other structural reports on the group 4 metallacarboranes have been those of the zircona- and hafnacarboranes, 1-Cl-1-THF-2,2′-$(SiMe_3)_2$-3,3′-$(R)_2$-1,1′-*commo*-M(2,3-$C_2B_4H_4)_2$ (M = Zr, Hf; R = $SiMe_3$, Me, H),[14] and our preliminary EPR/structural report on the mixed-ligand sandwich titanacarboranes, [*commo*-1-Cp-1-Ti-2,3-$(SiMe_3)_2$-2,3-$C_2B_4H_4]_2$ and *commo*-1-Cp-1-Cl-1-THF-1-Ti-2,3-$(SiMe_3)_2$-2,3-$C_2B_4H_4$.[15]

Herein, we report more detailed EPR data on [*commo*-1-Cp-1-Ti-2,3-$(SiMe_3)_2$-2,3-$C_2B_4H_4]_2$ (**1**, [CpTiCb]$_2$ (Cb = 2,3-$(SiMe_3)_2$-2,3-$C_2B_4H_4$)) and on the related [Li(TMEDA)]$_2$[1,1′-Ti-(2-Me-3-$SiMe_3$-2,3-$C_2B_4H_4)_2]_2$ (**5A**; [Li(TMEDA)]$_2$[$(Cb^*)_2$Ti]$_2$ (TMEDA = $Me_2NCH_2CH_2NMe_2$; Cb* = 2-Me-3-$SiMe_3$-2,3-$C_2B_4H_4$)) and on its one-electron oxidation product (**5B**), which was generated by controlled potential oxidation; the complexes were also characterized by UV/vis/NIR spectroscopic and electrochemical studies and, in the case of **1** and **5A**, by single-crystal X-ray studies. In addition, we report the structures and EPR measurements of the related monomeric Ti(III) compounds [Li(TMEDA)]$_2$[1-Cl-1,1′-Ti-(2,3-$(SiMe_3)_2$-2,3-$C_2B_4H_4)_2$] (**4**) and [1-(TMEDA)-1-Cl-1-Ti-2,4-$(SiMe_3)_2$-2,4-$C_2B_4H_4$] (**6**), the latter of which contains the isomeric 2,4-$C_2B_4H_4$ carborane ligand. The results of the chemical oxidation of [1-(Cp)-1-Ti-2-(R)-3-$(SiMe_3)$-2,3-$C_2B_4H_4)]_2$ (R = $SiMe_3$ (**1**), Me (**2**), H (**3**)) by $TiCl_4$ to produce the corresponding diamagnetic Ti(IV) species 1-(Cp)-1-(Cl)-1-(THF)-1-Ti-2-(R)-3-$(SiMe_3)$-2,3-$C_2B_4H_4$) (R = $SiMe_3$ (**7**), Me (**8**), H (**9**)) are also described, as well as the details of their NMR spectra and their solid state structures, as represented by **7**.

Experimental Section

Materials. The syntheses of 2-(R)-3-(trimethylsilyl)-2,3-dicarba-*nido*-hexaborane (**8**) (R = $SiMe_3$, Me, H) and their conversion to *closo-exo*-4,5-[$(\mu$-H$)_2$Li(TMEDA)]-1-Li(TMEDA)-2-(R)-3-$(SiMe_3)$-2,3-$C_2B_4H_4$ and 1,2-bis(trimethylsilyl)-1,2-dicarba-*closo*-hexaborane (**6**) followed the literature methods.[16] The "carbons apart" dilithiacarborane precursor *closo-exo*-5,6-[$(\mu$-H$)_2$Li(TMEDA)]-1-Li(TMEDA)-2,4-$(SiMe_3)_2$-2,4-$C_2B_4H_4$ was synthesized by the two-electron reduction of the corresponding dicarba-*closo*-hexaborane (**6**), as previously described.[17] Prior to use, Cp_2TiCl_2 and $TiCl_3$ (Strem) were heated to 130 °C, *in vacuo*, for 24 h to remove any traces of moisture and/or HCl. $TiCl_4$ was fractionated through vacuum traps held at 0, −78, and −196 °C, with the pure colorless liquid $TiCl_4$ being collected in the −78 °C trap. *tert*-Butyllithium, *t*-BuLi (1.7 M solution in pentane, obtained from Aldrich), was used as received. Benzene, TMEDA, and *n*-hexane were dried over NaH or Na metal and doubly distilled before use. The spectroscopic-grade solvents toluene, acetone, and 1,2-dichloroethane (DCE) were dried by distillation over potassium, Drierite, and CaH_2, respectively; oxygen was removed by several freeze/thaw cycles under vacuum. All other solvents were dried over 4−8 Å mesh molecular sieves (Aldrich) and were either saturated with dry argon or degassed before use. Unless otherwise noted, the manipulation of all compounds were done under oxygen-free anhydrous conditions using high-vacuum and/or standard Schlenk techniques under argon.

Spectroscopic Procedures. Proton, boron-11, carbon-13, and lithium-7 pulse Fourier transform NMR spectra, at 200, 64.2, 50.3, and 77.7 MHz, respectively, were recorded on an IBM-200 SY multinuclear NMR spectrometer. Infrared spectra were recorded on a Perkin-Elmer Model 1600 FT-IR spectrophotometer or a Nicolet Magna 550 FT-IR spectrophotometer. UV/vis/NIR absorption spectra were recorded on a Bruins Instruments Omega 10 spectrophotometer. Elemental analyses were determined by E+R Microanalytical Laboratory, Inc., Corona, NY.

(6) VanVleck, H. *The Theory of Electrical and Magnetic Susceptibilities*; Oxford University Press: London, 1932.
(7) Kahn, O. *Molecular Magnetism*; VCH: New York, 1993.
(8) Mabbs, F. E.; Collison, D. *Electron Paramagnetic Resonance of d Transition Metal Compounds*; Elsevier: Amsterdam, 1992.
(9) Samuel, E.; Harrod, J. F.; Gourier, D.; Dromzee, Y.; Robert, F.; Jeannin, Y. *Inorg. Chem.* **1992**, *31*, 3252.
(10) Xin, S.; Harrod, J. F.; Samuel, E. *J. Am. Chem. Soc.* **1994**, *116*, 11562.
(11) (a) Grimes, R. N. In *Comprehensive Organometallic Chemistry II*; Abel, E. W., Stone, F. G. A., Wilkinson, G., Eds.; Elsevier Science, Ltd.: Oxford, England, 1995; Vol. 1, Chapter 9. (b) Hosmane, N. S.; Maguire, J. A. In *Electron-Deficient Boron and Carbon Clusters*; Olah, G. A., Wade, K., Williams, R. E., Eds.; Wiley: New York, 1991; Chapter 9. (c) Hosmane, N. S.; Maguire, J. A. *Adv. Organomet. Chem.* **1990**, *30*, 99. (d) Hosmane, N. S.; Maguire, J. A. *J. Cluster Science* **1993**, *4*, 297.
(12) (a) Crowther, D. J.; Baenziger, N. C.; Jordan, R. F. *J. Am. Chem. Soc.* **1991**, *113*, 1455. (b) Jordan, R. F. *Makromol. Chem., Makromol. Symp.* **1993**, *66*, 121. (c) Jordan, R. F. New Organometallic Models for Ziegler−Natta Catalysts. In *Proceedings of the World Metallocene Conference*; Catalyst Consultants: Spring House, PA, 1993; p 89. (d) Bowen, D. E.; Jordan, R. F.; Rogers, R. D. *Organometallics* **1995**, *14*, 3630. (e) Kreuder, C.; Jordan, R. F.; Zhang, H. *Organometallics* **1995**, *14*, 2993.
(13) (a) Stockman, K. E.; Houseknecht, K. L.; Boring, E. A.; Sabat, M.; Finn, M. G.; Grimes, R. N. *Organometallics* **1995**, *14*, 3014. (b) Houseknecht, K. L.; Stockman, K. E.; Sabat, M.; Finn, M. G.; Grimes, R. N. *J. Am. Chem. Soc.* **1995**, *117*, 1163.
(14) (a) Thomas, C. J.; Jia, L.; Zhang, H.; Siriwardane, U.; Maguire, J. A.; Wang, Y.; Brooks, K. A.; Weiss, V. P.; Hosmane, N. S. *Organometallics* **1995**, *14*, 1365. (b) Zhang, H.; Jia, L.; Hosmane, N. S. *Acta Crystallogr., Cryst. Struct. Commun.* **1993**, *C49*, 453−456.
(15) Hosmane, N. S.; Wang, Y.; Zhang, H.; Maguire, J. A.; Waldhör, E.; Kaim, W.; Binder, H.; Kremer, R. K. *Organometallics* **1994**, *13*, 4156.
(16) (a) Hosmane, N. S.; Sirmokadam, N. N.; Mollenhauer, M. N. *J. Organomet. Chem.* **1985**, *279*, 359. (b) Hosmane, N. S.; Mollenhauer, M. N.; Cowley, A. H.; Norman, N. C. *Organometallics* **1985**, *4*, 1194. (c) Barreto, R. D.; Hosmane, N. S. *Inorg. Synth.* **1992**, *29*, 89. (d) Hosmane, N. S.; Sexena, A. K.; Barreto, R. D.; Maguire, J. A.; Jia, L.; Wang, Y.; Oki, A. R.; Grover, K. V.; Whitten, S. J.; Dawson, K.; Tolle, M. A.; Siriwardane, U.; Demissie, T.; Fagner, J. S. *Organometallics* **1993**, *12*, 3001.
(17) Zhang, H.; Wang, Y.; Saxena, A. K.; Oki, A. R.; Maguire, J. A.; Hosmane, N. S. *Organometallics* **1993**, *12*, 3933.

Table 1. Preparation of Titanacarboranes

compound	titanium reagent (amt: g, mmol)	amt of carborane precursor (g, mmol)	mp (°C)	yield[e] (g, mmol, %)
1	Cp_2TiCl_2 (0.78, 3.13)	0.73, 3.13[a]	250 (dec)	0.62, 0.94, 60
2	Cp_2TiCl_2 (9.00, 36.15)	6.27, 36.15[a]	210−215 (dec)	10.60, 19.50, 54
3	Cp_2TiCl_2 (3.37, 13.56)	2.16, 13.56[a]	170 (dec)	4.18, 8.09, 60
4	$TiCl_3$ (1.76, 11.33)	10.33, 22.26[b]	223−227 (dec)	3.24, 4.23, 38
5A	$TiCl_3$ (1.12, 7.27)	6.27, 14.54[b]	237 (dec)	3.21, 2.98, 41
6	$TiCl_3$ (0.84, 5.46)	2.53, 5.46[c]	177	0.91, 2.18, 40
7	$TiCl_4$ (0.29, 1.52)	0.50, 0.76[d]	155−160 (dec)	0.58, 1.31, 86
8	$TiCl_4$ (2.40, 12.65)	3.42, 6.28[d]	150−156 (dec)	2.77, 7.28, 58
9	$TiCl_4$ (0.31, 1.60)	0.42, 0.82[d]	148−152 (dec)	0.27, 0.73, 45

[a] Unsolvated *closo-exo*-Li-1-Li-2-(R)-3-($SiMe_3$)-2,3-$C_2B_4H_4$ (R = $SiMe_3$, Me or H). [b] *closo-exo*-4,5-[(μ-H)$_2$Li(TMEDA)]-1-Li[(TMEDA)-2-(R)-3-($SiMe_3$)-2,3-$C_2B_4H_4$ (R = $SiMe_3$, Me). [c] *closo-exo*-4,5-[(μ-H)$_2$Li(TMEDA)]-1-Li[(TMEDA)-2,4-($SiMe_3$)$_2$-2,4-$C_2B_4H_4$. [d] [*commo*-1-Cp-1-Ti(III)-2-(R)-3-($SiMe_3$)-2,3-$C_2B_4H_4$]$_2$ (R = $SiMe_3$ (**1**), Me (**2**), or H (**3**)). [e] Yield is based on dilithiacarborane or titanacarborane consumed.

Magnetic Susceptibility. Magnetic susceptibilities were measured between 14 K and room temperature with a MPMS Quantum Design SQUID magnetometer in a magnetic field of 1 T. The samples (~50 mg) were contained in gelatine capsules, the magnetization of which were determined in separate runs and subtracted. Corrections for core diamagnetism were not applied.

EPR Spectra and Cyclic Voltammetry. EPR spectra were recorded in glassy frozen solutions at 110 K with a Bruker ESP 300 X-band spectrometer equipped with a HP 5350B microwave frequency counter and a Bruker ER035M gaussmeter, calibrated with the perylene anion radical. For EPR measurements with the microwave field parallel to the magnetic field ($B_1 \parallel B_z$), a Bruker ER4116DM dual mode X-band resonator was used, otherwise a standard Bruker TMH 110 cavity was employed ($B_1 \perp B_z$). The parameters D, E, g_x, g_y, and g_z were calculated by fitting the literature formulae[18] to the experimental field values obtained from the spectra. Simulations of the $\Delta M_S = 1$ part of the spectra were performed with a computer program written by F. Neese (University of Konstanz).[19]

Cyclic voltammetry measurements were carried out in 0.1 M Bu_4NPF_6 solutions of acetone for [Li(TMEDA)]$_2$[(Cb*)$_2$Ti]$_2$ (**5A**) or 1,2-dichloroethane for [CpTiCb]$_2$ (**1**); the different solvents were employed for solubility reasons. A three-electrode configuration (glassy carbon working electrode, Pt counter electrode, and Ag/AgCl reference electrode) and an EG & G M273 potentiostat and function generator were used. Potentials against the ferrocene/ferrocenium couple, $Fc^{0/+}$, were obtained by external calibration, due to the reactivity of the compounds toward ferrocene.

The mixed-valence [(Cb*)$_2$Ti]$_2^-$ species, **5B**, was generated for *intra muros* EPR spectroscopy by controlled potential oxidation in an acetone/0.1 M Bu_4NPF_6 solution, with a three-electrode capillary (platinum working and counter electrode, silver wire as the pseudoreference electrode).

Synthetic Procedures. All syntheses were carried out in Pyrex glass round-bottom flasks of 100 mL capacity, equipped with magnetic stirring bars and high-vacuum Teflon valves. After their initial purifications, nonvolatile substances were manipulated in either a drybox or an evacuable glovebag under an atmosphere of dry nitrogen. All known compounds among the products were identified by comparing their IR and ^{1}H NMR spectra with those of authentic samples.

Synthesis of Mixed-Ligand Bent-Sandwich Cyclopentadienyl−Ti(III)−Carboranes, [1-(Cp)-1-Ti-2-(R)-3-($SiMe_3$)-2,3-$C_2B_4H_4$)]$_2$ (R = $SiMe_3$ (1), Me (2), H(3)). Except for the quantities used, the procedures in the syntheses of compounds 1−3 were identical. Therefore, only a typical synthesis will be described; the details of quantities used, product yields, and certain physical properties of 1−3 are summarized in Table 1.

A previously weighed sample of the unsolvated dilithiacarborane *closo-exo*-Li-1-Li-2-(R)-3-($SiMe_3$)-2,3-$C_2B_4H_4$ (R= $SiMe_3$, Me, H) was dissolved in a 1:1 solvent mixture of dry benzene and *n*-hexane (20 mL), and this solution was slowly poured into the benzene solution of anhydrous Cp_2TiCl_2 in a 100 mL reaction flask, with constant stirring at 0 °C over a period of 30 min. The resulting brown mixture was stirred at 0 °C for 5 h and then at room temperature for an additional 8 h. During this period, the reaction mixture turned from red to a green turbid solution. The heterogeneous product mixture was then filtered through a frit, and the residue was washed repeatedly with anhydrous benzene. The solid that remained on the frit after repeated washings was identified by qualitative analysis as LiCl (not measured) and was discarded. All of the volatiles, including solvents, were removed from the filtrate by vacuum distillation, and a green solid was collected, which was later recrystallized from a dry benzene solution to obtain air-sensitive deep green crystals that were identified as [*commo*-1-Cp-1-Ti(III)-2-(R)-3-($SiMe_3$)-2,3-$C_2B_4H_4$]$_2$ (R = $SiMe_3$ (**1**), Me (**2**), H (**3**)). The volatiles were fractionated through traps held at 0, −45, −78, and −196 °C; the trap at 0 °C collected a syrupy liquid, identified by NMR and IR spectroscopy as $(Cp)_2$ (0.124 g, 1.251 g, or 0.530 g, respectively).[20] Anal. Calcd (found) for $C_{26}H_{54}B_8Si_4Ti_2$ (**1**): C, 47.26 (47.64); H, 8.18 (8.16). Anal. Calcd (found) for $C_{22}H_{42}B_8Si_2Ti_2$ (**2**): C, 48.48 (48.28); H, 7.77 (7.69). Anal. Calcd (found) for $C_{20}H_{38}B_8Si_2Ti_2$ (**3**): C, 46.47 (46.31); H, 7.41 (7.67). The infrared spectral data with selected assignments for **1**−**3** are presented in Table 2.

Synthesis of Bent-Sandwich Ti(III)−Carboranes, Monomeric [Li(TMEDA)]$_2$ [*commo*-1,1′-Ti(Cl)-{2,3-($SiMe_3$)$_2$-2,3-$C_2B_4H_4$}$_2$] (4), and Dimeric [Li(TMEDA)]$_2$ [*commo*-1,1′-Ti-{2-(Me)-3-($SiMe_3$)-2,3-$C_2B_4H_4$}$_2$]$_2$ (5A). Except for the quantities used, the procedures in the synthesis of **4** and **5A** were identical. Therefore, only a typical synthesis will be described, with the details of quantities used, product yields, and certain physical properties being summarized in Table 1.

To a 100 mL flask containing a benzene solution of previously weighed anhydrous $TiCl_3$, a benzene solution of the TMEDA-solvated dilithiacarborane *closo-exo*-4,5-[(μ-H)$_2$Li-(TMEDA)]-1-Li[(TMEDA)-2-(R)-3-($SiMe_3$)-2,3-$C_2B_4H_4$ (R = $SiMe_3$, Me) was slowly added at 0 °C with constant stirring over a period of 30−40 min. The resulting mixture was stirred at room temperature for 12 h, during which time the mixture turned to a dark brown turbid solution. This mixture was then filtered through a frit, *in vacuo*, and the residue was washed repeatedly with anhydrous benzene; the combined filtrate/washings were then concentrated under vacuum to yield a dark brown semisolid. This solid was washed repeatedly with anhydrous *n*-hexane to obtain a dark solid, which was recrystallized from a benzene solution to yield an air-sensitive dark

(18) Reference 8, pp 476−478, eqs 11.34−11.40.

(19) Neese, F. Diploma Thesis; University of Konstanz, Konstanz, Germany, 1993.

(20) Hedaya, E.; McNeil, D. W.; Schissel, P.; McAdoo, D. J. *J. Am. Chem. Soc.* **1968**, *90*, 5284.

Table 2. Infrared Absorptions (cm^{-1}, C_6H_6 vs C_6H_6)[a]

compound	absorption
1	3089 (ss), 3033 (sm), 2954 (sm), 2897 (sm, ν(C−H)), 2547 (ss, ν(B−H)), 2276 (br, m), 1444 (sw), 1404 (sw), 1365 (sw), 1331 (sw), 1252 (ss), 1128 (sw), 1083 (sh), 1071 (ss), 1051 (sm), 834 (vs, s), 801 (ss), 682 (ss), 631 (sm), 597 (m, br)
2	2960 (vs), 2893 (ms), 2863 (w, ν(C−H)), 2556 (vs), 2536 (ms, ν(B−H)), 2393 (w), 2377 (w), 2352 (w), 1723 (w, br), 1448 (m), 1411 (m), 1365 (w), 1263 (ms), 1253 (vs), 1140 (w), 1094 (m, br), 1018 (ms), 880 (ms), 839 (vs), 803 (vs), 762 (m), 634 (m)
3	2959 (vs), 2933 (vs), 2897 (ms), 2680 (ms, ν(C−H)), 2558 (vs), 2531 (ms, ν(B−H)), 2369 (w, br), 2297 (w), 1634 (m), 1608 (m, br), 1410 (vs), 1368 (vs), 1258 (vs), 1071 (vs), 1024 (vs), 878 (ms), 846 (vs), 810 (vs), 750 (m), 652 (w)
4	3098 (vs), 3078 (vs), 3046 (vs), 2894 (ms), 2842 (ms, ν(C−H)), 2526 (vs), 2473 (vs, ν(B−H)), 2388 (w), 2328 (ms), 2217 (ms), 1966 (vs), 1851 (vs), 1762 (m), 1677 (ms), 1631 (w), 1525 (ms), 1486 (vs), 1394 (vs), 1361 (ms), 1295 (ms), 1249 (vs), 1190 (ms), 1038 (vs), 953 (ms), 841 (vs), 683 (vs)
5A	3092 (vs), 3072 (vs), 2908 (m), 2894 (ms, ν(C−H)), 2657 (ms), 2576 (m), 2598 (ms, ν(B−H)), 2388 (w), 2328 (ms), 2217 (ms), 1966 (vs), 1815 (vs), 1532 (vs), 1486 (vs), 1400 (ms), 1177 (ms), 1038 (vs), 854 (ms), 782 (m), 683 (vs)
6	2966 (vs), 2920 (vs), 2854 (vs, ν(C−H)), 2547 (vs, ν(B−H)), 2357 (w), 2121 (w, br), 1729 (m), 1637 (w), 1559 (ms), 1467(vs), 1382 (vs), 1271 (vs), 1094 (vs), 1022 (ms), 845 (vs), 810 (ms), 767 (w), 652 (w), 577 (w, br)
7	2956 (vs, s), 2898 (ms, ν(C−H)), 2580 (ms), 2542 (vs, ν(B−H)), 2305 (w, br), 2200 (w), 1904 (ms), 1805 (w, br), 1520 (w), 1482 (ms), 1406 (ms), 1330 (m, br), 1258 (vs, s), 1090 (vs), 1008 (vs, s), 928 (w), 832 (vs), 815 (vs), 800 (vs), 715 (m), 620 (w), 500 (w, br), 399 (vs)
8	2971 (vs), 2938 (vs), 2867 (vs, ν(C−H)), 2595 (vs, ν(B−H)), 2356 (w), 2265 (w), 2103 (m, br), 1941 (m), 1643 (w), 1553 (ms), 1507 (ms), 1456 (vs), 1391 (m), 1261 (vs), 1164 (m), 1106 (vs), 951 (w), 918 (w), 853 (vs), 756 (m), 627 (m), 556 (w, br)
9	2967 (vs), 2898 (ms), 2859 (ms, ν(C−H)), 2591 (ms), 2578 (vs, ν(B−H)), 2363 (m), 2278 (vs), 2128 (m, br), 1900 (w, br), 1626 (w), 1548 (ms), 1522 (ms), 1457 (vs), 1365 (m), 1333 (vs), 1261 (vs, s), 1104 (vs), 1026 (vs), 981 (m), 857 (m), 811 (vs), 756 (w), 570 (w, br), 505 (vs)

[a] Legend: v = very, s = strong or sharp, m = medium, w = weak, sh = shoulder, and br = broad.

green crystalline solid identified as [Li(TMEDA)]$_2$[*commo*-1,1′-Ti(Cl)-{2,3-($SiMe_3$)$_2$-2,3-$C_2B_4H_4$}$_2$] (**4**), or green crystals of the dimeric titanacarborane, [Li(TMEDA)]$_2$[*commo*-1,1′-Ti-{2-(Me)-3-($SiMe_3$)-2,3-$C_2B_4H_4$}$_2$]$_2$ (**5A**). Anal. Calcd (found) for $C_{28}H_{76}B_8Si_4N_4TiClLi_2$ (**4**): C, 43.96 (43.73); H, 10.01 (9.69); N, 7.32 (6.95); Cl, 4.63 (4.88). Anal. Calcd (found) for $C_{36}H_{96}B_{16}Si_4N_4Ti_2Li_2$ (**5A**): C, 44.11 (44.41); H, 9.87 (9.86); N, 5.72 (5.78). The infrared spectral data with selected assignments for **4** and **5A** are presented in Table 2.

Synthesis of the Half-Sandwich Ti(III)−Carborane 1-(TMEDA)-1-Cl-1-Ti-2,4-($SiMe_3$)$_2$-2,4-$C_2B_4H_4$ (6). In a manner similar to that described above, a freshly prepared sample of *closo-exo*-4,5-[(μ-H)$_2$Li(TMEDA)]-1-Li[(TMEDA)-2,4-($SiMe_3$)$_2$-2,4-$C_2B_4H_4$ was reacted with anhydrous $TiCl_3$, in 1:1 stoichiometry in dry benzene, with constant stirring at 0 °C. The resulting mixture was stirred overnight at room temperature to give a brown turbid solution. The product mixture was then filtered through a frit, *in vacuo*, and the residue was washed repeatedly with dry benzene. The filtrate and washings were combined and the solvent was removed by pumping to produce a dark residue that was then extracted with hexane. The hexane solution was concentrated under vacuum to yield air-sensitive brown crystals that were identified as the half-sandwich titanacarborane 1-(TMEDA)-1-Cl-1-Ti(III)-2,4-($SiMe_3$)$_2$-2,4-$C_2B_4H_4$ (**6**). The titanacarborane was later recrystallized from a benzene solution to obtain X-ray quality crystals. Anal. Calcd (found) for $C_{14}H_{38}N_2B_4Si_2TiCl$ (**6**): C, 40.29 (40.05); H, 9.20 (9.27); N, 6.71 (6.54). The infrared spectral data with selected assignments for **6** are presented in Table 2.

Synthesis of The Diamagnetic Mixed-Ligand Cyclopentadienyl−Ti(IV)−Carboranes 1-(Cp)-1-(Cl)-1-(THF)-1-Ti-2-(R)-3-($SiMe_3$)-2,3-$C_2B_4H_4$) (R = $SiMe_3$ (7), Me (8), H (9)). The general procedures used in the syntheses of compounds **7**−**9** from their respective Ti(III) precursors (**1**, **2**, **3**) were identical. As above, only a typical synthesis will be described, with the details of quantities used, product yields, and certain physical properties being summarized in Table 1.

A previously weighed sample of the dimeric titanacarborane [*commo*-1-Cp-1-Ti(III)-2-(R)-3-($SiMe_3$)-2,3-$C_2B_4H_4$]$_2$ (R = $SiMe_3$ (**1**), Me (**2**), H (**3**)) was dissolved in 20 mL of a solvent mixture consisting of dry benzene (60%) and dry THF (40%). The flask containing this solution was cooled to −196 °C, and freshly distilled $TiCl_4$ was then condensed into the flask. The flask was slowly warmed to room temperature (25 °C) over a period of 1−2 h, and then the mixture was stirred constantly for 24 h. During this period, the solution became turbid and turned from green/blue to brown. The heterogeneous product mixture was filtered through a frit, *in vacuo*, to collect a blue crystalline solid, which, after repeated washings with anhydrous *n*-hexane, was identified by elemental analysis as the reduced titanium product $TiCl_3(THF)_3$.[21] Solvents from the combined filtrate and washings were removed under vacuum to obtain a reddish-brown residue, which was extracted by dry *n*-hexane. The resulting hexane solution was concentrated, *in vacuo*, to collect a dark red solid, which was recrystallized from a solution of benzene and hexane to obtain an air-sensitive dark red crystalline solid, identified as *commo*-1-Cp-1-Cl-1-THF-1-Ti-2-(R)-3-($SiMe_3$)-2,3-$C_2B_4H_4$ (R = $SiMe_3$ (**7**), Me (**8**), H (**9**)). Anal. Calcd (found) for $C_{17}H_{35}O_1B_4Si_2ClTi$ (**7**): C, 46.60 (46.49); H, 8.05 (8.01); Cl, 8.09 (8.11). $C_{15}H_{29}O_1B_4SiTiCl$ (**8**): C, 47.40 (47.61); H, 7.69 (7.61). Anal. Calcd (found) for $C_{14}H_{27}O_1B_4SiTiCl$ (**9**): C, 45.94 (46.01); H, 7.44 (7.49). The infrared spectral data with selected assignments for **7**−**9** are presented in Table 2. NMR data for **7**−**9** are presented in Table 3.

X-ray Analyses of [1-(Cp)-1-Ti-2,3-($SiMe_3$)$_2$-2,3-$C_2B_4H_4$]$_2$ (1), [Li(TMEDA)]$_2$ [*commo*-1,1′-Ti(Cl)-{2,3-($SiMe_3$)$_2$-2,3-$C_2B_4H_4$}$_2$] (4), [Li(TMEDA)]$_2$ [*commo*-1,1′-Ti-{2-(Me)-3-($SiMe_3$)-2,3-$C_2B_4H_4$}$_2$]$_2$ (5A), 1-(TMEDA)-1-Cl-1-Ti-2,4-($SiMe_3$)$_2$-2,4-$C_2B_4H_4$ (6), and 1-(Cp)-1-(Cl)-1-(THF)-1-Ti-2,3-($SiMe_3$)$_2$-2,3-$C_2B_4H_4$) (7). Dark green to dark brown crystals of **1**, **5A**, and **6** and a dark red crystal of **7**, coated with mineral oil, were mounted on a Siemens R3m/V diffractometer under a low-temperature nitrogen stream. The pertinent crystallographic data and parameters for data collection are summarized in Table 4. Final unit cell parameters were obtained by a least-squares fit of the angles of 24−30 accurately centered reflections in the 2θ range from 16° to 32.0°. Intensity data were collected at 220−230 K using graphite-monochromatized Mo Kα (λ = 0.710 73 Å) radiation. For each compound, three standard reflections were monitored during the data collection and did not show any significant changes in intensity. All data sets were corrected for Lorentz and polarization effects and for absorption. The structures were solved by direct methods and subsequent difference Fourier syntheses using the SHELXTL-Plus package.[22,23] Full-matrix least-squares refinement was performed for each structure. Scattering factors, as well as anomalous-dispersion correction

(21) Manzer, L. E. *Inorg. Synth.* **1982**, *21*, 135. Thiele, K. H.; Schäfer, W. *Z. Anorg. Allg. Chem.* **1970**, *381*, 205.
(22) Sheldrick, G. M. *Structure Determination Software programs;* Siemens X-ray Analytical Instruments Corp., Inc.: Madison, WI, 1990.
(23) Sheldrick, G. M. *SHELXL93*, program for the refinement of Crystal Structures; University of Göttingen, Göttingen, Germany, 1993.

Table 3. FT-NMR Spectral Data

compound	data (δ)
1−**6**[a]	
7	^{1}H NMR: 6.08 (s, Cp), 3.33 (br, THF), 1.29 (br, THF), 0.58 (s, $SiMe_3$) ^{11}B NMR: 46.10 (d, 1 basal BH, ^1J(B−H) = 117 Hz), 32.99 (d, 2 basal BH, ^1J(B−H) = 117 Hz), −8.62 (d, 1 apical BH, ^1J(B−H) = 162 Hz) ^{13}C NMR: 122 (s, cage C), 117.33 (d, Cp, J = 178 Hz), 75.14 (t, CH_2, J = 106 Hz), 24.77 (t, CH_2, J = 106 Hz), 3.12 (q, $SiMe_3$, J = 117 Hz)
8	^{1}H NMR: 6.68 (s, Cp), 3.52 (br, THF), 2.68 (s, Me), 1.40 (br, THF),0.90 (s, $SiMe_3$) ^{11}B NMR: 45.86 (d, 1 basal BH, ^1J(B−H) = 121 Hz), 31.41 (d, 2 basal BH, ^1J(B−H) = unresolved), −5.64 (d, 1 apical BH, ^1J(B−H) = 158 Hz)
9	^{1}H NMR: 6.44 (s, cage CH), 6.16 (s, Cp), 3.45 (br, THF), 1.37 (br, THF), 0.24 (s, $SiMe_3$) ^{11}B NMR: 43.12 (d, 1 basal BH, ^1J(B−H) = 107 Hz), 28.10 (d, 2 basal BH, ^1J(B−H) = unresolved), −8.28 (d, 1 apical BH, ^1J(B−H) = 142 Hz)

[a] No useful NMR data obtained for these paramagnetic Ti(III) compounds.

Table 4. Crystal Data[a] for Titanacarboranes 1, 5A, 6 and 7

	1	**5A**	**6**	**7**
formula	$C_{26}H_{54}B_8Si_4Ti_2$	$C_{42}H_{102}B_{16}N_4Si_2Li_2Ti_2{\cdot}C_6H_6$	$C_{14}H_{38}N_2B_4Si_2ClTi{\cdot}C_6H_6$	$C_{17}H_{35}OB_4Si_2ClTi$
fw	661.4	1136.4	495.3	438.2
cryst syst	triclinic	triclinic	orthorhombic	monoclinic
space group	$P\bar{1}$	$P\bar{1}$	$P2_12_12_1$	$P2_1/n$
a (Å)	10.672(3)	10.849(2)	11.380(3)	8.358(3)
b (Å)	11.497(4)	12.506(3)	12.938(4)	10.311(4)
c (Å)	14.848(5)	14.630(3)	20.108(6)	27.515(9)
α (deg)	89.37(3)	91.02(2)	90.00	90
β (deg)	89.94(2)	111.71(2)	90.00	92.54(3)
γ (deg)	90.82(2)	106.25(2)	90.00	90
V, (Å^3)	1822(1)	1754.2(7)	2961(2)	2349(1)
Z	2	1	4	4
D_{calcd} (Mg/m^3)	1.206	1.076	1.111	1.229
abs coeff (mm^{-1})	0.587	0.329	0.470	0.580
cryst dimens (mm)	0.30 × 0.15 × 0.20	0.30 × 0.25 × 0.l0	0.20 × 0.25 × 0.30	0.30 × 0.20 × 0.15
scan type	$\omega/2\theta$	$\omega/2\theta$	$\omega/2\theta$	$\omega/2\theta$
scan speed in ω (min, max)	5.0, 30.0	5.0, 30.0	6.0, 30.0	6.0, 30.0
2θ range (deg)	3.5−40.0	3.5−44.0	3.5−44.0	3.5−42.0
T (K)	230	220	220	230
decay (%)	0	0	0	0
no. data collected	3723	4573	2074	2762
no. obsd reflns, $F > 6.0\sigma(F)$	2337	3289	1764	1804
no. params refined	361	343	271	235
GOF	1.58	1.53	1.41	1.18
$\Delta\rho$ (max, min, e/Å^3)	0.33, −0.42	0.44, −0.31	0.34, −0.25	0.29, −0.26
R^b	0.055	0.045	0.043	0.036
R_w	0.070	0.063	0.055	0.048

[a] Graphite-monochromatized Mo Kα radiation, λ = 0.710 73 Å. [b] $R = \sum||F_o| - |F_c||/\sum|F_o|$, $R_w = [\sum w(F_o - F_c)^2/\sum w(F_o)^2]^{1/2}$, and $w = 1/[\sigma^2(F_o) + 0.001(F_o)^2]$.

for heavy atoms, were taken from ref 24. Both **1** and **5A** possess a crystallographic center of symmetry, which is located at the midpoint of Ti···Ti(a). A benzene molecule was found in the crystal lattice of **5A** and **6**. The methyl and methylene H atoms of all four structures were calculated using a riding model. Cage H atoms were located in difference Fourier maps and were not refined. The final values of R and R_w are listed in Table 4, and the atomic coordinates are given in the Supporting Information (Table S-1), and selected interatomic distances and angles are listed in Table 5.

X-ray crystallographic data were also collected on the monomeric chlorotitanacarborane, **4**. However, disorder in the lithium-solvating TMEDA molecules and in the trimethylsilyl carbons prevented the complete refinement of its structure. Only the atomic coordinates of this compound are included in the Supporting Information.

Results and Discussion

Synthesis. The reaction of Cp_2TiCl_2 with the unsolvated "carbons adjacent" dilithium compounds *closo-exo*-Li-1-Li-2-(R)-3-($SiMe_3$)-2,3-$C_2B_4H_4$ (R= $SiMe_3$, Me, H) produced the corresponding mixed-ligand sandwich titanacarboranes, [*commo*-1-Cp-1-Ti(III)-2-(R)-3-($SiMe_3$)-2,3-$C_2B_4H_4$]$_2$ (R = $SiMe_3$ (**1**), Me (**2**), H (**3**)) in yields of 60%, 54%, and 60%, respectively (see Table 1). Scheme 1 outlines these syntheses and the others contained in this report. In both the synthesis of the mixed-ligand sandwich Ti(III) complexes **1**−**3** and their subsequent oxidation to the corresponding Ti(IV) complexes **7**−**9**, the driving forces are most likely the stabilities of the respective Ti(III) products, as well as the dihydrofulvalene formed in the syntheses of **1**−**3**. Attempts to synthesize directly a Ti(IV) mixed-ligand sandwich complex from the reaction of the neutral *nido*-carboranes and Cp*$TiMe_3$, following the method of Jordan,[12e] gave complex mixtures of products that could neither be separated nor characterized. Therefore, most of the synthetic effort has involved the direct syntheses of Ti(III) complexes using $TiCl_3$ as the metalating agent. The products of the reactions with $TiCl_3$ with the different dilithiacarborane compounds depended on steric factors arising from the nature of the cage-carbon substituents and the location of the cage-carbons in the C_2B_3 bonding face of the carborane ligand (see Scheme 1). When the "carbons adjacent" bis(trimethylsilyl)-

(24) *International Tables For X-ray Crystallography*; Kynoch Press: Birmingham, U.K., 1974; Vol. IV.

Table 5. Bond Lengths (Å) and Bond Angles (deg)[a]

Bond Lengths

Compound **1**

Ti(1)−Cnt(11)	1.964	Ti(1)−Cnt(13)	2.039	Ti(2)−B(23A)	2.414(8)	Ti(2)−B(24A)	2.512(8)
Ti(2)−Cnt(12)	1.976	Ti(2)−Cnt(14)	2.029	C(11)−C(12)	1.506(8)	C(11)−B(15)	1.571(10)
Ti(1)−C(11)	2.344(6)	Ti(1)−C(12)	2.316(6)	C(11)−B(16)	1.671(9)	C(12)−B(13)	1.541(10)
Ti(1)−B(13)	2.367(8)	Ti(1)−B(14)	2.455(8)	C(12)−B(16)	1.755(9)	B(13)−B(14)	1.626(11)
Ti(1)−B(15)	2.392(8)	Ti(1)−C(Sl)	2.343(11)	B(13)−B(16)	1.769(11)	B(14)−B(15)	1.607(11)
Ti(1)−C(52)	2.352(8)	Ti(1)−C(53)	2.324(11)	B(14)−B(16)	1.781(12)	B(15)−B(16)	1.796(11)
Ti(1)−C(54)	2.332(10)	Ti(1)−C(55)	2.359(13)	C(2l)−C(22)	1.505(8)	C(2l)−B(25)	1.569(10)
Ti(1)−B(13A)	2.365(8)	Ti(1)−B(14A)	2.516(9)	C(2l)−B(26)	1.694(10)	C(22)−B(23)	1.549(10)
Ti(2)−C(21)	2.359(7)	Ti(2)−C(22)	2.333(7)	C(22)−B(26)	1.728(10)	B(23)−B(24)	1.643(11)
Ti(2)−B(23)	2.391(8)	Ti(2)−B(24)	2.488(7)	B(23)−B(26)	1.770(11)	B(24)−B(25)	1.643(11)
Ti(2)−B(25)	2.377(8)	Ti(2)−C(61)	2.361(13)	B(24)−B(26)	1.808(12)	B(25)−B(26)	1.798(12)
Ti(2)−C(62)	2.360(10)	Ti(2)−C(63)	2.369(12)	Ti(1)···Ti(1a)	3.636(3)	Ti(2)···Ti(2a)	3.699(3)
Ti(2)−C(64)	2.365(11)	Ti(2)−C(65)	2.375(9)				

Compound **5A**

Ti−Cnt(51)	2.015	Ti−Cnt(52)	2.008	C(11)−C(31)	1.516(6)	C(12)−B(13)	1.541(6)
Ti−C(11)	2.383(5)	Ti−C(12)	2.439(4)	C(12)−B(16)	1.728(6)	B(13)−B(14)	1.653(6)
Ti−B(13)	2.438(5)	Ti−B(14)	2.434(5)	B(13)−B(16)	1.778(9)	B(14)−B(15)	1.644(8)
Ti−B(15)	2.405(6)	Ti−C(21)	2.365(4)	B(14)−B(16)	1.754(7)	B(15)−B(16)	1.774(7)
Ti−C(22)	2.359(5)	Ti−B(23)	2.440(5)	C(2l)−C(22)	1.483(5)	C(2l)−B(25)	1.555(6)
Ti−B(24)	2.490(5)	Ti−B(25)	2.412(4)	C(2l)−B(26)	1.697(6)	C(2l)−C(35)	1.515(5)
Ti−B(23A)	2.479(4)	Ti−B(24A)	2.533(4)	C(22)−B(23)	1.556(6)	C(22)−B(26)	1.760(5)
Li−B(14)	2.419(8)	Li−B(15)	2.444(7)	B(23)−B(24)	1.641(6)	B(23)−B(26)	1.778(5)
Li−B(25)	2.773(10)	Li−N(41)	2.111(6)	B(24)−B(25)	1.643(6)	B(24)−B(26)	1.781(7)
Li−N(42)	2.148(8)	C(11)−C(12)	1.483(6)	B(25)−B(26)	1.792(8)	Ti···Ti(a)	3.731(2)
C(11)−B(15)	1.556(5)	C(11)−B(16)	1.716(6)				

Compound **6**

Ti−Cnt(6)	1.948	Ti-Cl	2.307(2)	C(11)−B(15)	1.574(9)	C(11)−B(16)	1.717(10)
Ti−C(11)	2.322(6)	Ti−B(12)	2.338(7)	B(12)−C(13)	1.545(9)	B(12)−B(16)	1.758(11)
Ti−C(13)	2.347(6)	Ti−B(14)	2.407(7)	C(13)−B(14)	1.544(9)	C(13)−B(16)	1.712(10)
Ti−B(15)	2.413(7)	TI−N(Sl)	2.280(5)	B(14)−B(15)	1.682(10)	B(14)−B(16)	1.751(11)
Ti−N(52)	2.270(5)	C(11)−B(12)	1.543(9)	B(15)−B(16)	1.757(11)		

Compound **7**

Ti−Cnt(71)	1.991	Ti−Cnt(72)	2.075	Ti−C(55)	2.410(6)	Ti−O(61)	2.183(3)
Ti−Cl	2.344(2)	Ti−C(11)	2.413(4)	C(11)−C(12)	1.493(6)	C(11)−B(15)	1.561(7)
Ti−C(12)	2.431(5)	Ti−B(13)	2.410(6)	C(11)−B(16)	1.747(7)	C(12)−B(13)	1.574(7)
Ti−B(14)	2.392(6)	Ti−B(15)	2.389(5)	C(12)−B(16)	1.728(7)	B(13)−B(14)	1.644(8)
Ti−C(51)	2.405(6)	Ti−C(52)	2.372(6)	B(13)−B(16)	1.763(8)	B(14)−B(15)	1.680(8)
Ti−C(53)	2.388(5)	Ti−C(54)	2.377(5)	B(14)−B(16)	1.765(8)	B(15)−B(16)	1.770(8)

Bond Angles

Compound **1**

Cnt(11)−Ti(l)−Cnt(13)	142.8	Cnt(12)−Ti(2)−Cnt(14)	142.5	C(11)−B(16)−B(15)	53.7(4)	C(12)−B(16)−B(15)	92.2(5)
C(12)−C(11)−B(15)	112.6(5)	C(12)−C(11)−B(16)	66.8(4)	B(13)−B(16)−B(15)	92.7(5)	B(14)−B(16)−B(15)	53.4(4)
B(15)−C(11)−B(16)	67.2(5)	C(11)−C(12)−B(13)	107.7(5)	C(22)−C(2l)−B(25)	110.6(5)	C(22)−C(2l)−B(26)	65.1(4)
C(11)−C(12)−B(16)	61.1(4)	B(13)−C(12)−B(16)	64.5(4)	B(25)−C(2l)−B(26)	66.7(5)	C(2l)−C(22)−B(23)	109.7(5)
C(12)−B(13)−B(14)	108.6(6)	C(12)−B(13)−B(16)	63.6(4)	C(2l)−C(22)−B(26)	62.7(4)	B(23)−C(22)−B(26)	65.1(5)
B(14)−B(13)−B(16)	63.1(5)	B(13)−B(14)−B(15)	105.9(6)	C(22)−B(23)−B(24)	108.6(6)	C(22)−B(23)−B(26)	62.3(4)
Ti(1)−B(14)−B(16)	92.8(4)	B(13)−B(14)−B(16)	62.4(5)	B(24)−B(23)−B(26)	63.8(5)	B(23)−B(24)−B(25)	103.6(6)
B(15)−B(14)−B(16)	63.8(5)	C(11)−B(15)−B(14)	104.9(6)	B(23)−B(24)−B(26)	61.5(4)	B(25)−B(24)−B(26)	62.6(5)
C(11)−B(15)−B(16)	59.1(4)	B(14)−B(15)−B(16)	62.8(5)	C(2l)−B(25)−B(24)	107.2(6)	C(2l)−B(25)−B(26)	60.0(4)
C(11)−B(16)−C(12)	52.1(3)	C(11)−B(16)−B(13)	91.3(5)	B(24)−B(25)−B(26)	63.2(5)	C(2l)−B(26)−C(22)	52.2(4)
C(12)−B(16)−B(13)	51.9(4)	C(11)−B(16)−B(14)	93.7(5)	C(2l)−B(26)−B(23)	92.3(5)	C(22)−B(26)−B(23)	52.6(4)
C(12)−B(16)−B(14)	93.3(5)	B(13)−B(16)−B(14)	54.5(4)				

Compound **5A**

Cnt(5l)−Ti−Cnt(52)	138.9	B(14)−Li−B(15)	39.5(2)	C(11)−B(16)−B(15)	52.9(2)	C(12)−B(16)−B(15)	92.6(3)
B(14)−Li−B(25)	76.1(3)	B(15)−Li−B(25)	86.8(2)	B(13)−B(16)−B(15)	95.5(4)	B(14)−B(16)−B(15)	55.6(3)
B(14)−Li−N(41)	108.4(3)	B(15)−Li−N(41)	129.6(4)	C(22)−C(2l)−B(25)	113.0(3)	C(22)−C(2l)−B(26)	66.8(2)
B(25)−Li−N(41)	129.1(4)	B(14)−Li−N(42)	155.9(4)	B(25)−C(2l)−B(26)	66.7(3)	C(2l)−C(22)−B(23)	109.4(3)
B(15)−Li−N(42)	116.5(4)	B(25)−Li−N(42)	110.7(3)	C(2l)−C(22)−B(26)	62.4(2)	B(23)−C(22)−B(26)	64.5(2)
N(4l)−Li−N(42)	85.7(3)	C(12)−C(11)−B(15)	112.8(3)	C(22)−B(23)−B(24)	107.1(3)	C(22)−B(23)−B(26)	63.3(2)
C(12)−C(11)−B(16)	64.9(3)	B(15)−C(11)−B(16)	65.5(2)	B(24)−B(23)−B(26)	62.6(3)	B(23)−B(24)−B(25)	105.2(3)
C(11)−C(12)−B(13)	110.6(3)	C(11)−C(12)−B(16)	64.1(3)	B(23)−B(24)−B(26)	62.4(3)	B(25)−B(24)−B(26)	63.0(3)
B(13)−C(12)−B(16)	65.6(3)	C(12)−B(13)−B(14)	106.2(4)	C(2l)−B(25)−B(24)	105.0(3)	C(2l)−B(25)−B(26)	60.4(3)
C(12)−B(13)−B(16)	62.3(3)	B(14)−B(13)−B(16)	61.4(3)	B(24)−B(25)−B(26)	62.3(3)	C(2l)−B(26)−C(22)	50.8(2)
B(13)−B(14)−B(15)	105.8(3)	B(13)−B(14)−B(16)	62.8(3)	C(2l)−B(26)−B(23)	91.0(3)	C(22)−B(26)−B(23)	52.2(2)
B(15)−B(14)−B(16)	62.8(3)	C(11)−B(15)−B(14)	104.6(3)	C(2l)−B(26)−B(24)	93.7(3)	C(22)−B(26)−B(24)	93.2(3)
C(11)−B(15)−B(16)	61.6(2)	B(14)−B(15)−B(16)	61.6(3)	B(23)−B(26)−B(24)	54.9(2)	C(2l)−B(26)−B(25)	52.8(3)
C(11)−B(16)−C(12)	51.0(2)	C(11)−B(16)−B(13)	90.8(3)	C(22)−B(26)−B(25)	91.0(3)	B(23)−B(26)−B(25)	93.9(3)
C(12)−B(16)−B(13)	52.1(2)	C(11)−B(16)−B(14)	93.7(3)	B(24)−B(26)−B(25)	54.7(3)		
C(12)−B(16)−B(14)	94.4(3)	B(13)−B(16)−B(14)	55.8(3)				

Table 5 (Continued)

			Compound **6**				
Cnt(6)−Ti−Cl	120.6	Cnt(6)−Ti−N(51)	126.7	C(13)−B(14)−B(16)	62.2(4)	B(15)−B(14)−B(16)	61.5(4)
Cnt(6)−Ti−N(52)	123.5	Cl−Ti−N(51)	99.4(2)	C(11)−B(15)−B(14)	103.7(5)	C(11)−B(15)−B(16)	61.7(4)
Cl−Ti−N(52)	98.5(2)	N(5l)−Ti−N(52)	78.1(2)	B(14)−B(15)−B(16)	61.1(4)	C(11)−B(16)−B(12)	52.7(4)
B(12)−C(11)−B(15)	112.3(5)	B(12)−C(11)−B(16)	65.0(4)	C(11)−B(16)−C(13)	92.1(5)	B(12)−B(16)−C(13)	52.9(4)
B(15)−C(11)−B(16)	64.4(4)	C(11)−B(12)−C(13)	106.1(5)	C(11)−B(16)−B(14)	95.2(5)	B(12)−B(16)−B(14)	94.0(5)
C(11)−B(12)−B(16)	62.3(4)	C(13)−B(12)−B(16)	62.0(4)	C(13)−B(16)−B(14)	52.9(4)	C(11)−B(16)−B(15)	53.9(4)
B(12)−C(13)−B(14)	112.4(5)	B(12)−C(13)−B(16)	65.1(4)	B(12)−B(16)−B(15)	94.9(5)	C(13)−B(16)−B(15)	95.6(5)
B(14)−C(13)−B(16)	64.8(4)	C(13)−B(14)−B(15)	105.6(5)	B(14)−B(16)−B(15)	57.3(4)		
			Compound **7**				
Cnt(7l)−Ti−Cl	107.9	Cnt(7l)−Ti−O(61)	107.7	B(13)−B(14)−B(16)	62.2(3)	B(15)−B(14)−B(16)	61.8(3)
Cnt(72)−Ti−Cl	107.2	Cnt(72)−Ti−O(61)	103.7	C(11)−B(15)−B(14)	106.2(4)	C(11)−B(15)−B(16)	62.9(3)
Cnt(7l)−Ti−Cnt(72)	131.6	Cl−Ti−O(61)	91.4(l)	B(14)−B(15)−B(16)	61.5(3)	C(11)−B(16)−C(12)	50.9(3)
C(12)−C(11)−B(15)	111.2(4)	C(12)−C(11)−B(16)	63.9(3)	C(11)−B(16)−B(13)	92.5(4)	C(12)−B(16)−B(13)	53.6(3)
B(15)−C(11)−B(16)	64.4(3)	C(11)−C(12)−B(13)	111.4(4)	C(11)−B(16)−B(14)	95.2(4)	C(12)−B(16)−B(14)	95.1(4)
C(11)−C(12)−B(16)	65.2(3)	B(13)−C(12)−B(16)	64.4(3)	B(13)−B(16)−B(14)	55.6(3)	C(11)−B(16)−B(15)	52.7(3)
C(12)−B(13)−B(14)	106.4(4)	C(12)−B(13)−B(16)	62.1(3)	C(12)−B(16)−B(15)	92.1(4)	B(13)−B(16)−B(15)	96.3(4)
B(14)−B(13)−B(16)	62.3(3)	B(13)−B(14)−B(15)	104.7(4)	B(14)−B(16)−B(15)	56.7(3)		

[a] Cnt(11), Cnt(12): centroids of C_2B_3 rings of **1**. Cnt(13), Cnt(14): centroids of Cp rings of **1**. Cnt(51), Cnt(52): centroids of C_2B_3 rings of **5**. Cnt(6): centroid of C_2B_3 ring of **6**. Cnt(71): centroid of C_2B_3 ring of **7**. Cnt(72): centroid of Cp ring of **7**.

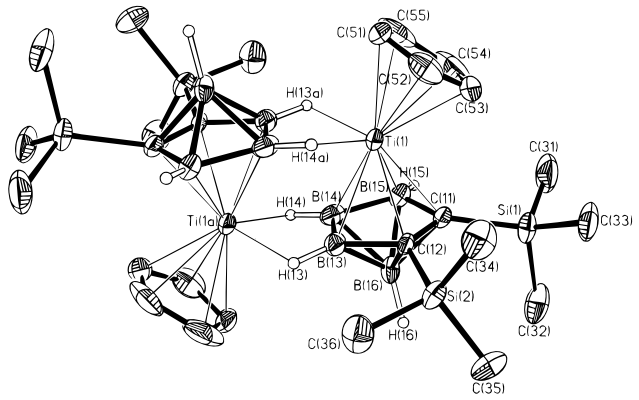

Figure 1. Perspective view of **1** showing the atom numbering scheme, with thermal ellipsoids drawn at the 40% probability level. The silylmethyl and the Cp H atoms are omitted for clarity.

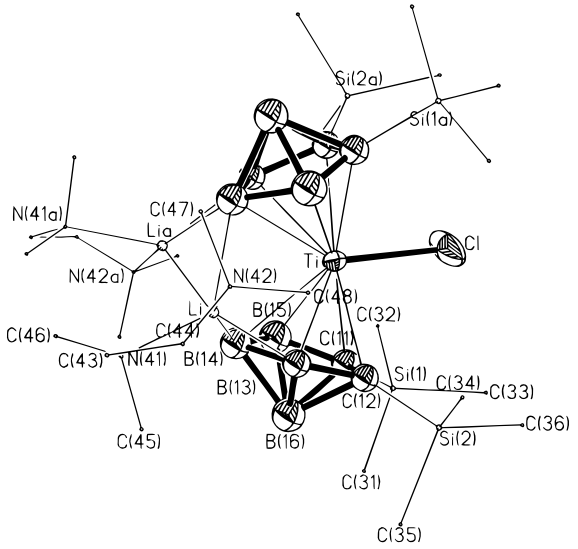

Figure 2. Perspective view of **4** showing the atom numbering scheme. For clarity, the *exo*-polyhedral $SiMe_3$ and $[Li(TMEDA)_2]$ moieties are drawn with circles of arbitrary radii.

carborane (Cb) was a reactant, only the monomeric full-sandwich chlorotitanacarborane, **4**, was formed, irrespective of the stoichiometry used in the reaction. Replacement of a $SiMe_3$ group with the smaller Me group afforded the $[(Cb^*)_2Ti]_2^{2-}$ dimer (**5A**) exclusively. In the same way, replacement of one of the Cb ligands with the smaller, isolobal and isoelectronic π-donor Cp ligand also resulted in dimer formation, giving the mixed-ligand dimers **1**−**3**. The only half-sandwich titanacarborane that could be formed was that of the carbons apart isomer, **6**. At present, it is not known exactly why the carbons apart and carbons adjacent carboranes should give such different products when reacted with $TiCl_3$. It could be that because of the intervening boron atom, the steric restrictions on additional coordination at the titanium imposed by the cage-carbon substituents would be somewhat tempered, allowing for the coordination of a chlorine atom and the large TMEDA molecule.

Crystal Structures of 1, 4, 5A, 6, and 7. The solid state structures of **1**, **5A**, **6**, and **7** are shown in Figures 1 and 3−5, respectively. Their crystallographic data are summarized in Table 4, atomic coordinates in the Supporting Information (Table S-1), and selected bond distances and bond angles are given in Table 5. Even though the structure of **4** could not be completely determined, the metal, cage atoms, and chlorine atom refined well and a partial structure is shown in Figure

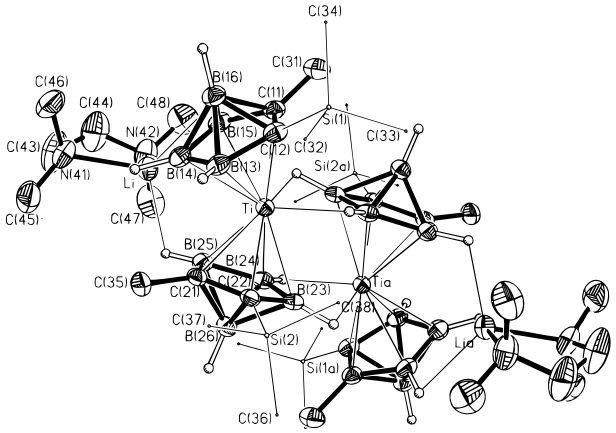

Figure 3. Perspective view of **5A** showing the atom numbering scheme, with thermal ellipsoids drawn at the 40% probability level. The methyl and methylene H atoms are omitted for clarity.

2. All structures show the titanacarboranes to be bent sandwich complexes, similar to those found in the Cp

Scheme 1

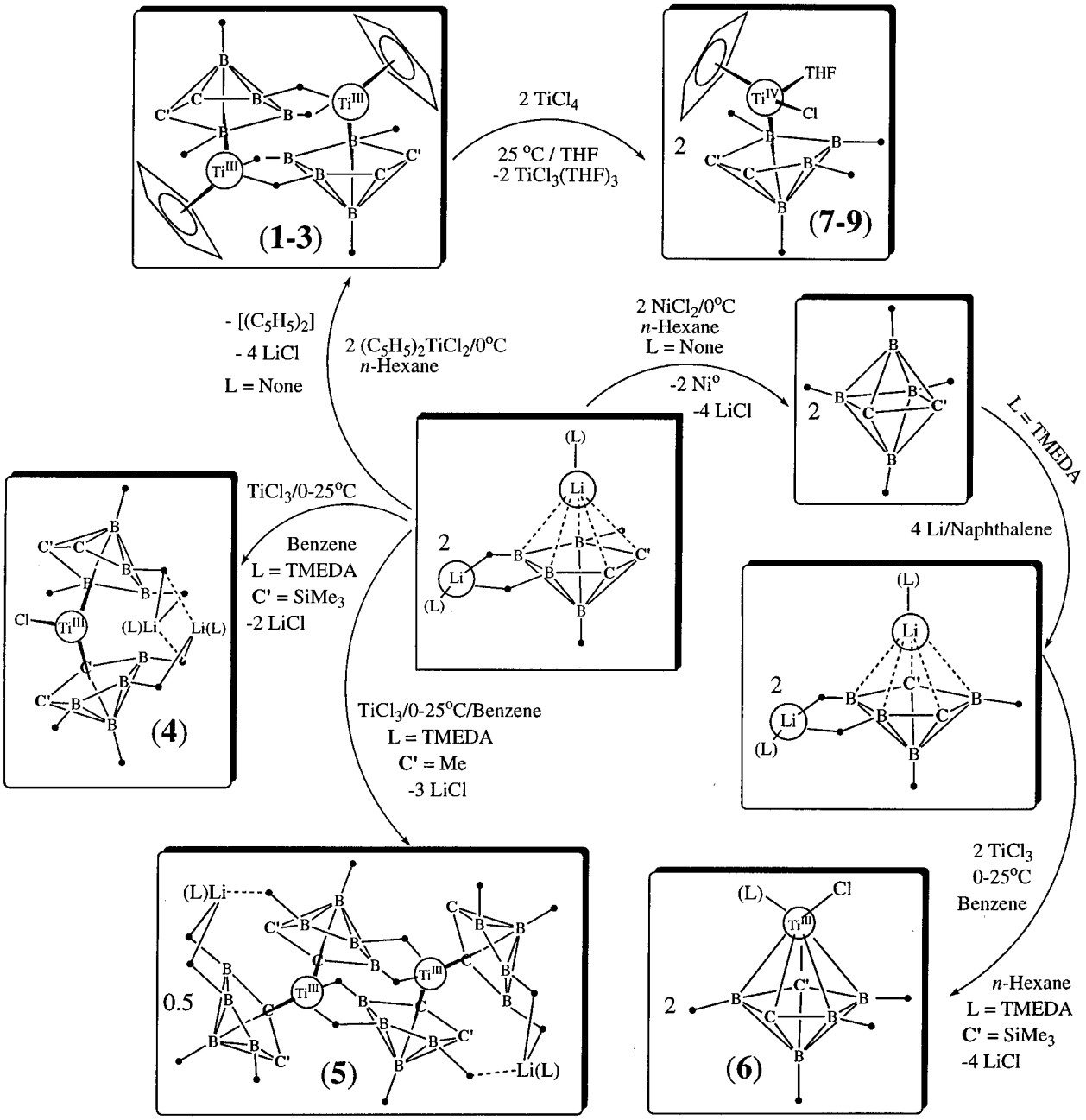

system.[4,9,25,26] The (ring centroid)−Ti−(ring centroid) bond angles in **1**, **4**−**7** range from 131.6° in **7** to 142.8° in **1**, which is well within the range of 130−144° found in the titanocenes[4,9,25,26] and similar to the analogous angles of 144.6° and 138.8° found by Jordan for the mixed-ligand complexes $[(Cp^*)Ti(NCMe_2)(C_2B_9H_{11})]$ and $[(Cp^*)Ti(NCMe_2)(MeCN)(C_2B_9H_{11})]$, respectively.[12e] A comparison of the distances between the Ti and the centroids of the Cp and C_2B_3 carborane rings in compounds **1**, **5A**, and **7** given in Table 5 reveals a surprising insensitivity to either the formal charge on the metals or the nature of the other ligands present. The average Ti−Cp distance of 2.054 ± 0.021 Å,[27] obtained from Table 5, is the same as the average distance of 2.054 ± 0.004 Å found in $[Cp_2TiCl]_2$[25a] and is close to the analogous distances found in a number of substituted titanocenes.[4,25,26] The average Ti−C_2B_3(centroid) distance of 1.996 ± 0.016 Å is close to the values of 2.02 and 1.91 Å found in the $Cp^*Ti(C_2B_9H_{11})$ mixed-ligand sandwich compounds of Jordan,[12e] as well as the Ti−C_2B_3(centroid) distance of 1.917 Å reported by Grimes for the cyclooctatetraene (COT)−titanacarborane 1-(η^8-C_8H_8)-1-Ti-2,3-$(Et)_2$-2,3-$C_2B_4H_4$.[28] The latter compound is of interest in that it, as well as its cyclopentadienide analogues,[29] are not bent but have a linear (ring

(25) (a) Jungst, R.; Sekutowski, D.; Davis, J.; Luly, M.; Stucky, G. D. *Inorg. Chem.* **1977**, *16*, 1645. (b) Peterson, J. L.; Dahl, L. F. *J. Am. Chem. Soc.* **1975**, *97*, 6422.

(26) Pattiasina, J. W.; Heeres, H. J.; Bolhuis, F. v.; Weetsma, A.; Teuben, J. H.; Spek, A. L. *Organometallics* **1987**, *6*, 1004.

(27) Whenever the average value of an experimental parameter is given, the indetermination cited is the average deviation.

(28) Swisher, R. G.; Sinn, E.; Grimes, R. N. *Organometallics* **1984**, *3*, 599.

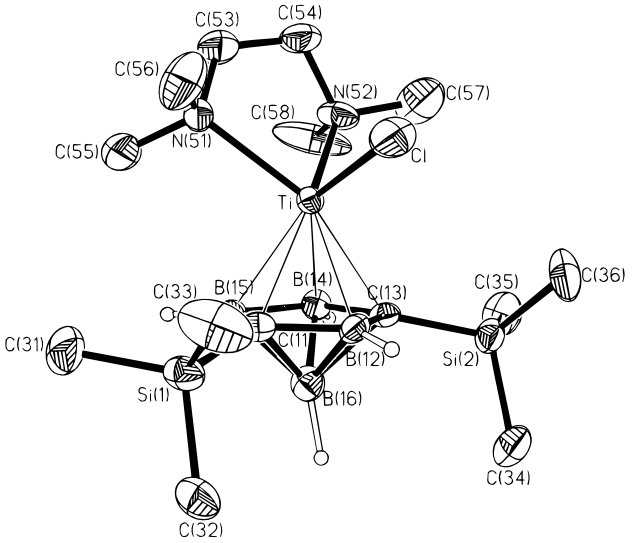

Figure 4. Perspective view of **6** showing the atom numbering scheme, with thermal ellipsoids drawn at the 40% probability level. The methyl and methylene H atoms are omitted for clarity.

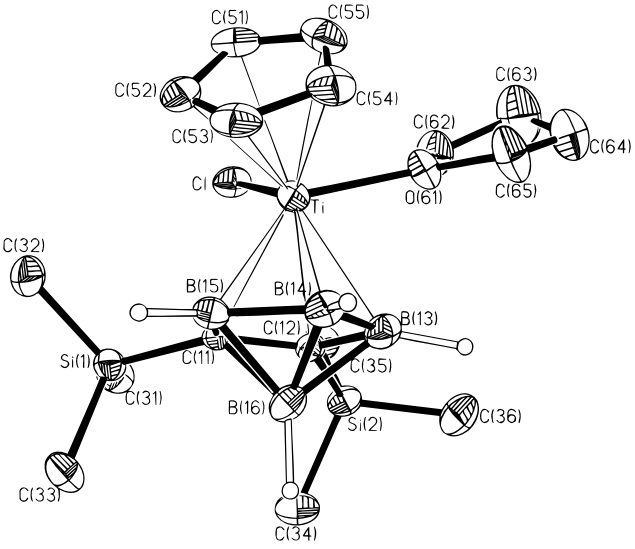

Figure 5. Perspective view of **7** showing the atom numbering scheme, with thermal ellipsoids drawn at the 40% probability level. The methyl, methylene, and Cp H atoms are omitted for clarity.

centroid)−Ti-(ring centroid) arrangement. It is not clear whether the linear structures found in the COT complexes are the result of the size of the $[C_8H_8]^{2-}$ ligand or the fact that it is a 10-electron donor. In the same way, while both steric and electronic effects are operative in determining the geometry of the full- and mixed-ligand titanacarborane sandwiches **1**−**7**, the relative importance of the two effects is not apparent. However, the influence of steric factors is readily seen in some of their structural features. The structures of the two full-sandwich complexes, **4** and **5A**, show that the C_2B_3 rings are twisted in such a way that the cage carbons, rather than borons, surround the open face of the bent sandwiches. For example, the dihedral angle between the line connecting the B(14)−Cnt(11) and Cnt(13)−B(24) lines in Figure 3 and their equivalents in Figure 4 are

(29) Koon, P. A.; Helmholdt, R. B. *J. Organomet. Chem.* **1984**, *263*, C43.

Table 6. *g* Factors of $[Li(TMEDA)]_2[Cb_2TiCl]$ (4) and [(2,4-Cb)TiCl(TMEDA)] (6) at 110 K

	$g_{\parallel}$	$g_{\perp}$	$g_{av} = (2g_{\perp} + g_{\parallel})/3$
	$[Li(TMEDA)]_2[Cb_2Ti\ Cl]$		
powder	1.892	1.985	1.954[a]
solution[b]	1.935	1.998	
	1.950	1.970	
solution[c]	1.935, 1.892, 1.874	1.985, 1.975	
	[Ti(2,4-Cb)Cl(TMEDA)]		
powder	1.86	1.958	1.93
solution	1.85	1.97	

[a] g_{iso} = 1.960 at 290 K, 4 mT peak-to-peak line width. [b] In toluene, dilute solution (1 mM). [c] In toluene, concentrated solution (1 M).

111.2° and 14.6°, respectively, where an angle of 0° would indicate that the cage-carbons were eclipsed and a 180° angle would be obtained if these atoms occupied positions opposite to each other. In most of the full-sandwich compounds where the carborane bonding faces are parallel, an angle of 180° is found,[30] while in bent-sandwich complexes, the rings are twisted.[31,32] Although the exact reason for this twisting is not known, it seems to be universal and does place the cage-carbons in close proximity to the other coordinating groups on the central metal. Therefore, steric restrictions imposed by the cage-carbon substituents will greatly influence the nature and extent of additional coordination on the central titanium atom. When the bis(trimethylsilyl)-substituted carboranes react with $TiCl_3$, the monomeric complex, **4**, is the only product, irrespective of the stoichiometry. As pointed out above, substitution of a $SiMe_3$ group by a sterically less demanding Me allows additional coordination to form the dimeric **5A**. This is similar to what is found in the titanocenes, where the substitution of a Cp ligand in $[Cp_2TiCl]_2$ by Cp* resulted in the isolation of the $[(Cp^*)_2TiCl]$ monomer.[25,26] Other properties may also be affected. For example, steric crowding by the $SiMe_3$ groups has been used to account for the lack of reactivity of the coordinated Cl and THF in the zirconacarborane anion [1-Cl-1-THF-2,2′,3,3′-$(SiMe_3)_4$-1,1′-*commo*-Zr(2,3-$C_2B_4H_4)_2]^-$.[31] It may well be that the use of different cage-carbon substituents and the locations of the cage-carbon atoms in the bonding face could be used to control the reactivites of these d^0 or d^1 bent-sandwich metallacarboranes. To this end, the half-sandwich carbons apart titanacarborane 1-Cl-1-(TMEDA)-2,4-$(SiMe_3)_2$-1,2,4-$TiC_2B_4H_4$ (**6**) was synthesized and its structure determined (see Figure 4). The reaction chemistry of this compound is currently being investigated in our laboratories, and the results of this study will be reported in the near future.

Spectroscopy. ESR Spectra and Magnetic Susceptibilities: Monomeric Compounds. Powder EPR spectra of $\{[Li(TMEDA)]_2[(Cb)_2TiCl]\}$ (**4**) and the carbons apart half-sandwich [(2,4-Cb)TiCl(TMEDA)] (**6**) at 110 K showed axial signals. Table 6 summarizes the *g* factors, which are typical for Ti(III) compounds.[33] In solution at room temperature, the EPR spectra of all compounds showed only one single broad line without resolved satellite coupling lines from ^{47}Ti ($I = {}^5/_2$, 7.4%

(30) For examples, see ref 11c.
(31) See ref 14a.
(32) Jia, L.; Zhang, H.; Hosmane, N. S. *Organometallics* **1992**, *11*, 2957.
(33) Goodman, B. A.; Raynor, J. B. *Adv. Inorg. Chem. Radiochem.* **1970**, *13*, 135.

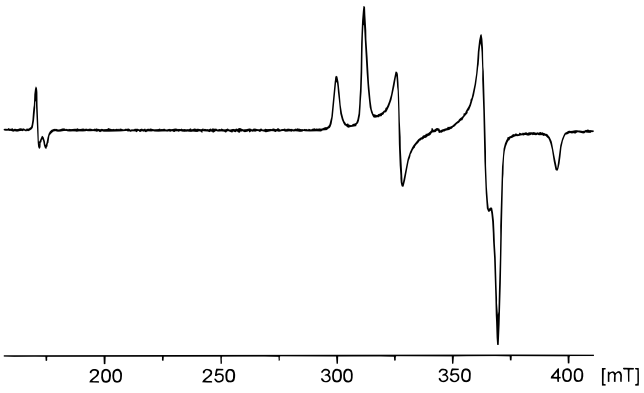

Figure 6. EPR spectrum of $[CpTiCb]_2$ (**1**) in glassy frozen toluene solution at 110 K ($B_1 \perp B_z$, $\nu_0 = 9.5703$ GHz).

Scheme 2

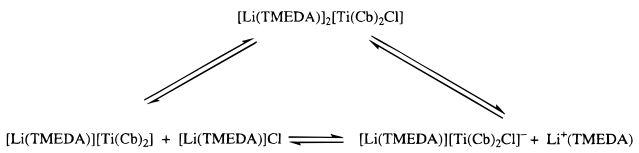

natural abundance) or ^{49}Ti ($I = {}^7/_2$, 5.4%). However, the EPR spectra of glassy frozen toluene solutions at 110 K showed the presence of several species. The spectra were concentration dependent, implying dissociation/aggregation processes. A probable explanation involves the formation of contact and/or solvent-separated ion pairs (Scheme 2). However, the absence of "half-field" transitions (see below) excludes the formation of stable inner-sphere Ti(III) dimers.

Dimeric Compounds. Triplet EPR Spectra. The Ti(III) dimers $[CpTiCb]_2$ (**1**) and $[Li(TMEDA)]_2$ $[(Cb^*)_2Ti]_2$ (**5A**) gave unusually well-resolved rhombic triplet ($S = 1$) EPR spectra in glassy frozen acetone and toluene solutions at 110 K. $\Delta M_S = 1$ transitions in the high-field region and $\Delta M_S = 2$ transitions (half-field transitions) in the low-field region were observed.[34] Figure 6 shows the textbook triplet EPR spectrum of $[CpTiCb]_2$ (**1**). The EPR spectrum of $[(Cb^*)_2Ti]_2^{2-}$ (**5A**$^{2-}$) is almost identical, but shows an additional weak signal in the center of the $\Delta M_S = 1$ transitions. EPR spectroelectrochemistry (see below) showed that this signal is most likely due to the presence of small amounts of the one-electron oxidized mixed-valence species $[(Cb^*)_2Ti]_2^-$ (**5B**). Additional measurements with the microwave field parallel to the magnetic field ($B_1 \parallel B_z$), where only $\Delta M_S = 2$ transitions can be observed,[35] confirmed the assignments (see Figure 7). The triplet EPR spectra clearly indicate rhombic symmetry, requiring the following spin Hamiltonian for analysis:[34,35]

$$H = \beta \boldsymbol{S} g \boldsymbol{B} + D(S_z^2 - {}^1/_3\, S^2) + E\,(S_x^2 - S_y^2) \quad (1)$$

D and E are the axial and rhombic components of the zero-field splitting (ZFS) tensor, $\boldsymbol{D}$. The component D can be interpreted as a measure of the deviation of the wave function from spherical symmetry (axis in z-direction), while E reflects the deviation between the x and y directions (rhombicity). Calculated and experimental field values of the $\Delta M_S = 1$ and $\Delta M_S = 2$ transitions, as indicated in the spectra shown in Figures 7 and 8, were obtained by fitting D, E, g_x, g_y, and g_z using the formulae summarized in ref 18. The results, listed in Tables 7 and 8 show an excellent agreement, which is also supported by a computer simulation[19] of the EPR spectra generated with these parameters (Figure 8).

Zero-Field Splitting Tensor, D. The axial and

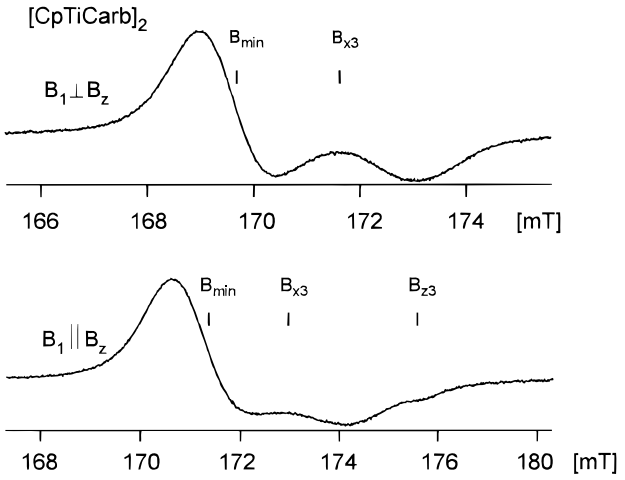

Figure 7. $\Delta M_S = 2$ transitions of $[CpTiCb]_2$ (**1**) in glassy frozen toluene solution at 110 K with $B_1 \perp B_z$ (top) and $B_1 \parallel B_z$ (bottom). Field values and microwave frequencies ν_0 are given in Table 7.

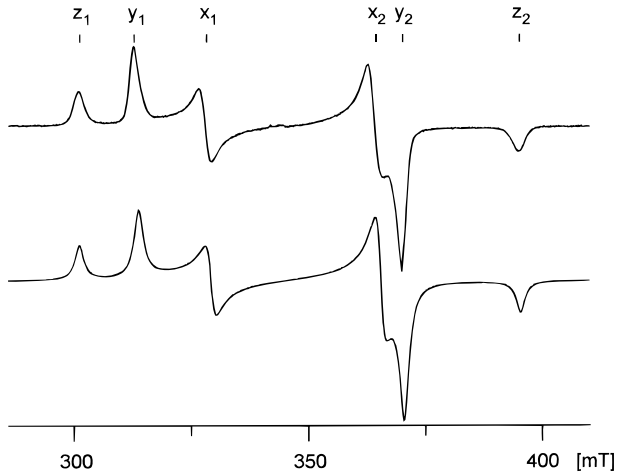

Figure 8. $\Delta M_S = 1$ transitions of $[CpTiCb]_2$ (**1**) in toluene solution at 110 K ($B_1 \perp B_z$), Experiment (top) and simulation (bottom). Field values are given in Table 7.

Table 7. Experimental and Calculated Field Positions of $\Delta M_S = 1$ Transitions[a]

	$[CpTiCb]_2$ (**1**)[b]		$[(Cb^*)_2Ti]_2^{2-}$ (**5A**$^{2-}$)[c]	
	exp	calcd	exp	calcd
B_{z1}	300.70 ± 0.05	300.70	312.4 ± 0.1	312.4
B_{y1}	312.50 ± 0.05	312.47	321.30 ± 0.05	321.30
B_{x1}	327.70 ± 0.05	327.71	336.7 ± 0.1	336.7
B_{x2}	364.2 ± 0.1	363.7	369.3 ± 0.1	368.6
B_{y2}	369.9 ± 0.1	369.6	375.00 ± 0.05	374.34
B_{z2}	394.8 ± 0.2	394.8	398.4 ± 0.1	398.4

[a] In mT; calculated according to ref 18. [b] $D = -0.0432$ cm^{-1}; $E = -0.00337$ cm^{-1}; $g_x = 2.0009$, $g_y = 1.9662$, $g_z = 1.9726$. $\nu_0 = 9.5703$ GHz. [c] $D = -0.0394$cm^{-1}; $E = -0.00337$ cm^{-1}; $g_x = 2.0044$, $g_y = 1.9646$, $g_z = 1.9759$. $\nu_0 = 9.7730$ GHz.

(34) Atherton, N. M. *Electron Spin Resonance*; Ellis Horwood, Ltd.: Sussex, England, 1973.

(35) (a) Dexheimer, S. L. Ph.D. Thesis, University of California, Berkeley, CA, 1990. (b) Dexheimer, S. L.; Klein, M. P. *J. Am. Chem. Soc.* **1992**, *114*, 2821. (c) Abragam, A.; Bleaney, B. *Electron Paramagnetic Resonance of Transition Metal Ions*; Clarendon Press: Oxford, England, 1970.

Table 8. Experimental and Calculated Field Positions of $\Delta M_S = 2$ Transitions[a]

	$[CpTiCb]_2$ (**1**)[b]				$[(Cb^*)_2Ti]_2^{2-}$ (**5A**$^{2-}$)[c]			
	$B_1 \perp B_z$ (9.5689 GHz)		$B_1 \parallel B_z$ (9.6512 GHz)		$B_1 \perp B_z$ (9.7727 GHz)		$B_1 \parallel B_z\nu_0$ (9.6833 GHz)	
	exp	calcd	exp	calcd	exp	calcd	exp	calcd
B_{min}	169.7 ± 0.1	170.5	171.2 ± 0.1	172.0	173.9 ± 0.2	174.4	172.3 ± 0.3	172.8
B_{x3}	171.7 ± 0.2	171.4	172.7 ± 0.2	172.9	175.9 ± 0.1	175.2	173.4 ± 0.3	173.5
B_{y3}	n.o.[d]	169.5	n.o.	171.0	n.o.	173.1	n.o.	171.5
B_{z3}	n.o.	173.8	175.1 ± 0.1	175.3	n.o.	177.7	n.o.	176.0

[a] In mT; calculated according to ref 18. [b] $D = -0.0432$ cm^{-1}; $E = -0.00337$ cm^{-1}; $g_x = 2.0009$; $g_y = 1.9662$; $g_z = 1.9726$. [c] $D = -0.0394$ cm^{-1}; $E = -0.00337$ cm^{-1}; $g_x = 2.0044$; $g_y = 1.9646$; $g_z = 1.9759$. [d] n.o. = not observed.

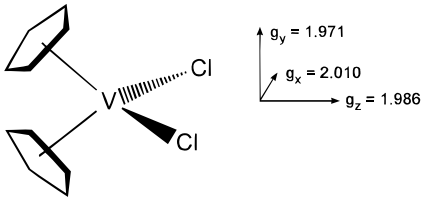

Figure 9. Molecular orientation of the ***g*** tensor in Cp_2VCl_2 as obtained from single-crystal EPR studies (refs 38 and 39).

rhombic ZFS parameters, D and E, are composed of dipolar and pseudodipolar contributions, D_d, E_d and D_{ps}, E_{ps},[9,36] according to eq 2. Pseudodipolar contributions

$$D = D_{ps} + D_d \; E = E_{ps} + E_d \tag{2}$$

arise from the admixture of an exchange-coupled excited state to the ground state by spin-orbit coupling and are generally expected to increase with a decreasing Ti−Ti distance, d.[9,36] Dipolar contributions arise from through-space interactions of the magnetic dipoles of the unpaired electrons and are only dependent on the distance d between them (eqs 3 and 4),[36] where D_d and E_d are in J and the Ti−Ti distance, d, is in m; $\mu_0 = 4\pi \times 10^{-7}$ VsA^{-1} m^{-1}; and $\beta = 9.2741 \times 10^{-24}$ Am^2. Accurate

$$D_d = -\frac{\mu_0 \beta^2}{4\pi 3d^3}\left(2g_z^2 + \frac{g_x^2 + g_y^2}{2}\right) \tag{3}$$

$$E_d = \frac{\mu_0 \beta^2}{4\pi 2d^3}(g_x^2 - g_y^2) \tag{4}$$

calculations of D_d and E_d from the Ti−Ti distance, d, require a knowledge of the molecular orientation of the principal axes of the ***g*** tensor. Because of the inversion symmetry of the dimers studied here, the g axes of the Ti centers should be colinear with each other and with the ZFS tensor ***D***.[37] Unfortunately, no Ti(III) species has as yet been subjected to a single-crystal EPR study. Therefore, a reference to the related mononuclear d^1 system Cp_2VCl_2, for which such studies have been performed,[38,39] is necessary. The molecular orientation of the g axes in Cp_2VCl_2 is given in Figure 9. A comparison of a large number of compounds of the type Cp_2VLL' showed that g factors are independent of L and L′, implying identical tensor orientations.[40] These results have also been transferred successfully to Ti(III) monomers[40] and dimers.[9,37]

Table 9 summarizes the D, E, and g components of $[(Cb^*)_2Ti]_2^{2-}$ (**5A**$^{2-}$), $[CpTiCb]_2$ (**1**), and other related compounds of similar structure and known Ti−Ti distances. In this table, the g axes have been reassigned tentatively according to the Cp_2VCl_2 reference system. A similar study was performed for $[Cp_2TiOR]_2$ (R = Me, Et) and $[Cp_2TiCl]_2$.[9] However, the assignments of the g values to the molecular directions in that study were erroneous, due to confusion in the assignment of the axes; the correct assignment was used in Table 9. Dipolar and pseudodipolar contributions to D and E, as calculated from eqs 2 and 3, are listed in Table 10.

The values of all ZFS parameters of $[(Cb^*)_2Ti]_2^{2-}$ and $[CpTiCb]_2$ lie well within the range of related compounds. However, a rather large g anisotropy, $g_x - g_z$, is observed, which might reflect the low symmetry of the coordination environment of the titanium (Table 10). Nonetheless, replacing Cp^- by a Cb^{2-} unit does not seem to have a large effect on the absolute values of the ZFS parameters. As expected, D and E generally decrease with increasing d. While D is mainly dipolar and E mainly pseudodipolar in character, the dipolar contribution to D decreases with increasing d whereas it increases for E. The dominant dipolar character of D, as opposed to the pseudodipolar character of E, has been explained assuming antiferromagnetic exchange interactions J_x (xz-plane) and ferromagnetic exchange interactions J_y (yz-plane).[9] For D, these interactions tend to cancel each other whereas they add up for the nonaxial component E.

If the observed trends are not coincidental, to a large extent D is determined by the Ti−Ti distance, d, whereas E depends on the nature of the bridging ligands which mediate the exchange interactions J_x and J_y. Predictions of the pseudodipolar contributions D_{ps} and E_{ps} are difficult due to the complex nature of the exchange interactions, which depend on the specific electronic situation in the bridges linking the two spin centers. This is illustrated by comparison of $[Cp_2Ti(OMe)]_2$ and $[Cp_2Ti(OEt)]_2$ and of $[CpTiCb]_2$ and $[(Cb^*)_2Ti]_2^{2-}$; despite the very similar Ti−Ti distances and bridging ligands within each pair, a rather large discrepancy in D, D_d, and D_{ps} is observed. The reasons are not very obvious and would justify further (i.e., single-crystal EPR) investigations.

Magnetic Susceptibility and Exchange Coupling. Magnetic susceptibility measurements between 14 and 300 K show antiferromagnetic coupling between the two unpaired d electrons in the dimer **1**. Fitting the curve with the Bleaney−Bowers equation yields $J = -45.8(2)$ cm^{-1}; Figure 10 shows the plot of the experimental magnetic susceptibility vs temperature

(36) Pilbrow, J. R. *Transition Ion Electron Paramagnetic Resonance*; Clarendon Press: Oxford, England, 1990.
(37) Francesconi, L. C.; Corbin, D. R.; Clauss, A. W.; Hendrickson, D. N.; Stucky, G. D. *Inorg. Chem.* **1981**, *20*, 2059.
(38) Petersen, J. L.; Dahl, L. F. *J. Am. Chem. Soc.* **1975**, *97*, 6422.
(39) Petersen, J. L.; Dahl, L. F. *J. Am. Chem. Soc.* **1975**, *97*, 6433.
(40) Casey, A. T.; Raynor, J. B. *J. Chem. Soc. Dalton Trans.* **1983**, 2057.

Table 9. Zero-Field Splitting Parameters *D* and *E* (cm^{-1}) and *g* Components of Ti(III) Dimers[a]

compound	*D*	*E*	g_x	g_y	g_z	$g_x - g_y$	d_{Ti-Ti}[b]	ref
Cp_2VCl_2			2.010	1.971	1.986			16−18
$[(Ind)_2TiH]_2$[c]	−0.0433	−0.00816	1.9972	1.9604	1.9786	0.0186	3.2288(13)	7
$[Cp_2Ti(OMe)]_2$	−0.0446	−0.0069	2.0017	1.9647	1.9803	0.0214	3.358(2)	6
$[Cp_2Ti(OEt)]_2$	−0.0463	−0.0066	1.9975	1.9584	1.9760	0.0215	3.358(2)	6
$[CpTiCb]_2$	−0.0432	−0.00337	2.0009	1.9662	1.9726	0.0283	3.699(3)	this work
$[(Cb^*)_2Ti]_2^{2-}$	−0.0394	−0.00337	2.0044	1.9646	1.9759	0.0285	3.731(2)	this work
$[Cp_2TiCl]_2$	−0.0375	−0.000(5)	2.000	1.979	1.986	0.014	3.958(3)	6

[a] Assignment of *g* components to molecular axes according to Cp_2VCl_2 (Figure 9); *z* axis corresponds to the Ti−Ti axis. [b] Ti−Ti distance in Å. [c] Ind = tetrahydroindenyl.

Table 10. Dipolar (D_d, E_d) and Pseudodipolar (D_{ps}, E_{ps}) Contributions to the Zero-Field Splitting Parameters *D* and *E* (cm^{-1})[a]

compound	d[b]	D_d	D_{ps}	E_d	E_{ps}	ref
$[(Ind)_2TiH]_2$	3.2288(13)	−0.0503	+0.0070	−0.00094	−0.00722	7
$[Cp_2Ti(OMe)]_2$	3.358(2)	−0.0448	+0.0002	−0.00084	−0.00606	6
$[Cp_2Ti(OEt)]_2$	3.358(2)	−0.0446	−0.0018	−0.0009	−0.0057	6
$[CpTiCb]_2$	3.699 (3)	−0.0342	−0.0090	−0.00060	−0.00277	this work
$[(Cb^*)_2Ti]_2^{2-}$	3.731 (2)	−0.0327	−0.0067	−0.00066	−0.00271	this work
$[Cp_2TiCl]_2$	3.958(3)	−0.0275	−0.0100	−0.0003	+0.0003	6

[a] Calculated from eqs 2−4 with the parameters listed in Table 10. [b] Crystallographic Ti−Ti distance in Å.

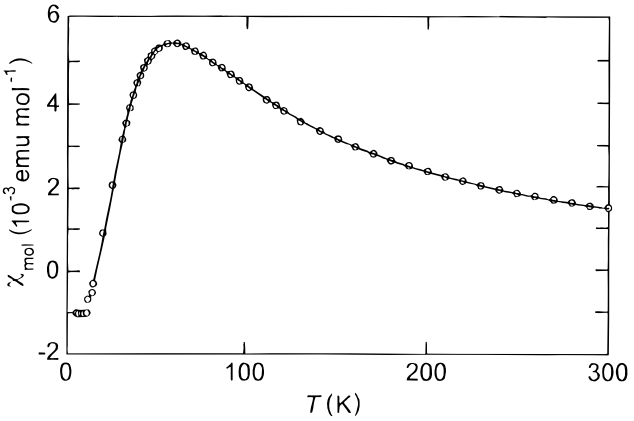

Figure 10. Plot of the experimental magnetic susceptibility (open circles) vs temperature and the fit with the Bleaney−Bowers equation (solid line) for **1**.

Scheme 3

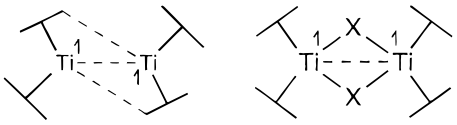

and the fit with the Bleaney−Bowers equation. Magnetic exchange coupling constants have been reported for $[Cp_2Ti(OMe)]_2$ ($J = -268$ cm^{-1}) and $[Cp_2TiCl]_2$ ($J = -111$ cm^{-1}).[9] Although the exact mechanism for the coupling interaction is not known, the significantly smaller *J* value for the carborane dimer **1** indicates that the large carborane bridging ligand is less effective in propagating magnetic exchange interactions between the spin centers, specifically, there are no single atoms available as easy pathways for superexchange (see Scheme 3). A comparison with the EPR data shows that these are less sensitive to the coordination environment and mainly depend on the distance, *d*, between the unpaired electrons. On the other hand, magnetic exchange coupling constants reflect the specific orientation and electronic situation of the pathway through which the exchange interaction is mediated. Sample decomposition prevented the collection of reliable magnetic susceptibility data on **5A**.

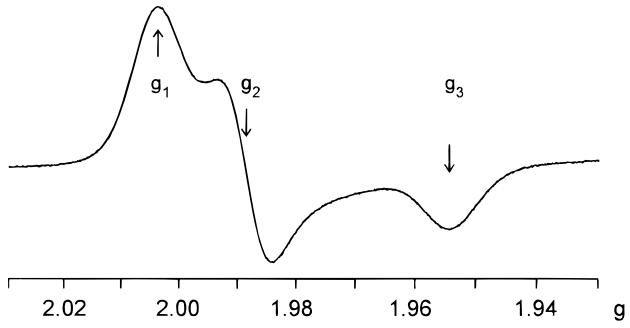

Figure 11. EPR spectrum of electrochemically generated $[(Cb^*)_2Ti]_2^-$ (**5B**) in glassy frozen solution (acetone/0.1 M Bu_4NPF_6) at 110 K.

Electrochemistry, EPR Spectroelectrochemistry, and Absorption Spectra. The cyclovoltammogram of $[(Cb^*)_2Ti]_2^{2-}$ (**5A**$^{2-}$) in acetone/0.1 M Bu_4NPF_6 shows a reversible oxidation wave at $E_{1/2} = -0.60$ V vs $Fc^{0/+}$ ($\Delta E_{pp} = 80$ mV), leading to the mixed-valence species $[(Cb^*)_2Ti]_2^-$ (**5B**). A second but irreversible wave follows at +0.05 V vs $Fc^{0/+}$ (anodic peak potential and 100 mV/s scan rate). The $[CpTiCb]_2$ (**1**), which is insoluble in acetone, could only be oxidized irreversibly in DCE/0.1 M Bu_4NPF_6 at a peak potential of −0.30 V vs $Fc^{0/+}$.

The different electrochemical behavior of the two dimers is attributed to differing charges, the oxidation of the dianionic $[(Cb^*)_2Ti]_2^{2-}$ (**5A**$^{2-}$) being favored both with respect to the potential and the stability of the one-electron oxidized product. The difference of 0.65 V between the two anodic features of $[(Cb^*)_2Ti]_2^{0/-/2-}$ suggests a comproportionation constant $K_c = [-]^2/[0][2-] = 10^{\Delta E/0.059V}$ of more than 10^{10}. Even larger K_c values were reported for oxo-bridged Ti(IV)/Ti(III) species.[41]

The Ti(IV)/Ti(III) mixed-valence species $[(Cb^*)_2Ti]_2^-$ (**5B**) was also generated electrochemically *in situ* by controlled potential electrolysis for EPR characterization. Figure 11 shows the resulting doublet ($S = {}^1/_2$) EPR spectrum[42] of the glassy frozen acetone solution

(41) Jeske, P.; Wieghardt, K.; Nuber, B. *Inorg. Chem.* **1994**, *33*, 47.
(42) Castro, S. L.; Streib, W. E.; Huffman, J. C.; Christou, G. *J. Chem. Soc., Chem. Commun.* **1996**, 2177.

of the mixed-valence compound at 110 K, which exhibits a distinctly rhombic pattern: $g_1 = 2.0038$, $g_2 = 1.9886$, and $g_3 = 1.9541$. These g values are identical with those of the "impurity" in the center of the $\Delta M_S = 1$ transitions of $[(Cb^*)_2Ti]_2^{2-}$ (**5A**$^{2-}$, see above).

The question of localized or delocalized valencies in the mixed-valent $[(Cb^*)_2Ti]_2^-$ must remain open; no ^{47}Ti and ^{49}Ti hyperfine coupling features could be observed, and the expected coupling would be in the order of 1 mT.[33] Due to the extreme sensitivity of the solutions to traces of air and water, UV/vis/NIR spectroelectrochemical studies in search of a long-wavelength intervalence transition were unsuccessful. However, the rhombic EPR pattern and the large g anisotropy of $[(Cb^*)_2Ti]_2^-$ as opposed to that of the $\Delta M_S = 1$ part of $[(Cb^*)_2Ti]_2^{2-}$ ($\Delta g = 0.0498$ vs 0.0285) suggest a delocalized situation for the mixed-valence compound **5B**. In a Ti(III)/Ti(IV) species, as opposed to a Ti(+3.5)/Ti(+3.5) species, the (axial) symmetry and g values would be expected to resemble those of Ti(III) monomers or dimers. A Ti(+3.5)/Ti(+3.5) model is also supported by the rapid disintegration of the Ti(IV)/Ti(IV) state.

Solutions of $[CpTiCb]_2$ (**1**) in toluene and of $[(Cb^*)_2Ti]_2^{2-}$ (**5A**$^{2-}$) in acetone are deep green and show very similar spectra, with absorption bands at 415 and 620 nm (broad) and a long-wavelength shoulder at ~750 nm. By comparison with $[(Me_3tacn)Ti(NCO)]_2(\mu\text{-O})$,[33] which has two ligand-field (LF) transitions at ~550 and 680 nm, the long-wavelength features can also be assigned to LF transitions. The shift to lower energy may then be explained by the weaker ligand field of the carborane ligands as opposed to the μ-oxo bridge.

Conclusions. The structures of the full-sandwich Ti(III) and Ti(IV) carborane complexes have been found to be sensitive to the nature of the substituent groups on the cage-carbon atoms of the carboranes. The solid state structures of these bent-sandwich complexes show that the carborane cages are twisted so that cage-carbons surround the open face of the compounds. Large cage-carbon substituents inhibit additional coordination of the central metal, giving rise to monomeric compounds with low coordinate titanium atoms, such as found in **4**, while sterically less demanding substituents allow for additional coordination and dimer formation. The Ti(III) dimers gave well-resolved triplet EPR spectra whose g components and ZFS parameters lie well within the range of values found for other dimeric Ti(III) complexes. Low-temperature magnetic susceptibility measurements of dimer **1** showed antiferromagnetic coupling with an unusually small magnetic exchange coupling constant.

Acknowledgment. Dedicated, with all best wishes, to Professor Herbert Binder of Universität Stuttgart, Germany, on the occasion of his 60th birthday. This work was supported in part by grants from the Texas Advanced Technology Program (003613006), the Robert A. Welch Foundation (N-1016 to N.S.H. and N-1322 to J.A.M.), the National Science Foundation (CHE-9400672), and the donors of the Petroleum Research Fund, administered by the American Chemical Society. Support from the Deutsche Forschungsgemeinschaft (DFG) and the Volkswagen Foundation is also gratefully acknowledged.

Supporting Information Available: Figure showing perspective view of the structure of **4** (Figure S-1) and tables of atomic coordinates for **1**, **4**, **5A**, **6**, and **7** (Table S-1), bond lengths and bond angles for **1** (Table S-2), **5A** (Table S-3), **6** (Table S-4), and **7** (Table S-5), anisotropic displacement parameters for **1**, **5A**, **6**, and **7** (Table S-6), and H-atom coordinates and isotropic displacement coefficients for **1**, **5A**, **6**, and **7** (Table S-7) (24 pages). Ordering information is given on any current masthead page.

OM960890K